Supplementary Table 1. Primers for BSH gene amplification.

Protein	Primer	Sequence
B. theta BSH	Bt_BSH_F	ATA GCT AGC ATG TGT ACG CGG GCG GTT TAC
B. theta BSH	Bt_BSH_R	ATC GCT CGA GCA TGA CTG GCG TTT CAA AC
B. longum BSH	Bl_BSH_F	GAT TGG CTA GCA TGT GCA CCG GCG TTC GT
B.longum BSH	Bl_BSH_R	GGG CTC GAG ACG TGC CAC TGA GAT TAA TTC

Supplementary Table 2. % deconjugation of each bile acid determined in experiments with a pool of four tauro conjugated bile acids.

		% deconjugation of TCA			% deconjugation of TβMCA			% deconjugation of TUDCA			% deconjugation of TDCA		
		replicate 1	replicate 2	replicate 3	replicate 1	replicate 2	replicate 3	replicate 1	replicate 2	replicate 3	replicate 1	replicate 2	replicate 3
Figure 2a, 2 hours													
Control		1.19	1.10	0.26	33.70	31.31	29.69	96.16	95.42	95.73	98.25	98.71	98.15
Compound 1		0.12	0.17	0.29	3.72	3.29	3.28	37.96	35.92	33.34	51.40	46.10	43.43
Compound 2		0.90	22.25	0.48	34.64	0.98	30.95	95.53	94.77	93.56	98.39	97.77	97.37
Compound 3		0.67	1.01	0.09	34.08	27.93	27.02	95.01	94.06	91.94	97.76	97.25	96.55
Compound 4		0.47	1.15	0.30	32.07	29.34	22.69	94.07	91.62	89.81	97.26	96.13	94.56
Compound 5		0.95	0.92	1.05	32.80	36.63	9.44	96.13	96.16	95.10	98.42	98.52	98.57
Compound 6		0.92	1.25	0.59	35.60	34.07	42.48	96.03	93.99	93.59	98.74	97.53	97.40
Compound 7		0.00	0.06	0.07	0.00	0.00	0.00	1.77	1.53	1.45	2.16	1.98	2.01
Compound 8		1.15	0.59	2.07	14.58	29.59	38.71	97.82	95.09	96.63	99.29	98.31	99.01
Riboflavin		1.37	0.06	0.69	37.87	30.51	33.21	99.21	94.73	94.97	99.69	97.30	97.98
CAPE		0.36	0.08	0.06	14.25	12.45	10.19	76.05	74.21	70.00	76.46	75.12	72.52
Figure 2a, 21 hours													
Control		2.93	3.44	1.16	61.21	71.43	55.90	99.06	99.21	99.02	97.10	97.36	94.86
Compound 1		0.12	0.17	0.15	3.18	4.28	3.11	34.40	41.24	37.45	45.18	51.87	45.19
Compound 2		0.21	2.67	2.13	27.46	61.90	51.76	96.86	99.36	98.17	93.10	98.34	96.06
Compound 3		1.08	1.44	2.82	38.49	45.51	59.04	97.70	99.19	99.48	93.30	97.89	97.49
Compound 4		1.50	0.85	1.80	47.65	32.41	43.47	98.54	97.31	97.80	95.87	95.61	96.21
Compound 5		4.41	3.75	3.05	70.08	68.59	63.03	99.58	99.62	99.25	98.66	99.29	97.94
Compound 6		2.57	0.00	1.90	64.01	0.30	61.81	99.32	53.74	99.44	98.26	62.13	98.29
Compound 7		0.00	0.09	0.00	0.00	0.00	0.00	0.32	1.81	1.09	0.45	2.25	0.53
Compound 8		1.90	3.94	2.71	60.01	69.30	60.40	99.39	99.62	99.58	97.93	99.68	98.41
Riboflavin		2.39	3.55	3.41	54.39	65.09	67.26	98.88	99.48	99.59	94.28	97.99	96.89
CAPE		0.74	0.09	1.11	25.75	3.08	37.00	93.76	59.73	96.84	91.61	54.27	94.84
Figure 2b, 2 hours													
Control		84.30	86.35	57.07	3.17	3.22	1.58	37.34	39.53	32.17	98.75	99.15	98.88
Compound 1		0.10	0.89	0.43	2.49	0.05	0.03	2.12	1.09	0.61	7.25	4.34	2.20
Compound 7		0.03	0.98	1.05	0.49	0.06	0.04	1.05	1.39	1.43	0.15	0.19	0.24
CAPE		68.68	55.04	54.30	2.05	1.81	1.50	26.95	25.15	24.35	93.93	93.63	93.26
Figure 2b, 21 hours													
Control		96.43	99.43	99.10	33.36	35.07	30.92	96.65	97.65	97.19	98.12	99.24	98.84
Compound 1		9.02	3.00	8.03	0.21	0.13	0.28	4.57	2.48	3.66	23.33	14.91	20.42
Compound 7		1.61	1.00	1.61	0.11	0.08	0.11	2.11	1.54	2.36	0.37	0.22	0.39
CAPE		98.46	97.65	98.90	25.75	19.28	23.96	93.63	92.01	93.28	97.84	98.03	97.42
Supplementary Figure 3a, 5 hours													
Control		0.09	2.13	2.50	53.21	51.95	55.87	99.76	99.80	99.71	99.92	99.94	99.94
Compound 1		0.25	0.00	0.21	4.42	4.47	3.37	38.73	40.02	35.99	52.56	51.54	45.63
Compound 2		0.38	1.34	1.77	43.58	51.12	45.91	99.47	99.51	99.47	99.85	99.91	99.57
Compound 3		0.85	2.89	1.97	46.39	56.31	44.08	99.39	99.60	99.06	99.83	99.91	99.75
Compound 4		0.40	1.92	1.29	26.17	45.65	37.57	98.43	98.54	97.17	99.59	99.50	99.01
Compound 5		2.33	3.50	1.92	54.06	53.97	50.71	99.64	99.74	96.67	99.94	99.95	99.86
Compound 6		0.55	1.62	2.39	44.48	50.02	51.09	99.61	99.41	99.67	97.07	99.88	99.89
Compound 7		0.00	0.00	0.00	0.00	0.00	0.00	1.27	1.43	1.05	1.60	2.00	1.32
Compound 8		2.91	2.99	2.29	60.02	57.01	54.60	99.94	99.79	99.79	99.96	99.96	99.91
Riboflavin		0.90	1.95	0.21	41.18	50.96	47.55	99.58	99.54	99.43	99.91	99.87	99.69
CAPE		0.29	0.77	0.05	23.21	24.76	20.62	89.91	91.34	88.49	90.81	91.46	89.67
Supplementary Figure 3b, 5 hours													
Control		100.00	97.74	100.00	7.67	8.47	7.83	63.76	67.92	64.49	99.80	99.86	99.77
Compound 1		4.13	4.57	4.31	0.10	0.11	0.11	2.44	2.49	2.64	9.85	11.26	11.96
Compound 7		0.88	1.09	1.15	0.05	0.04	0.04	1.39	1.34	1.51	0.15	0.17	0.17
CAPE		90.99	93.66	93.73	4.55	5.27	5.06	48.74	50.94	49.29	99.78	99.73	99.81

Supplementary Table 2. continued

		% deconjugation of TCA			% deconjugation of TβMCA			% deconjugation of TUDCA			% deconjugation of TDCA		
		replicate 1	replicate 2	replicate 3	replicate 1	replicate 2	replicate 3	replicate 1	replicate 2	replicate 3	replicate 1	replicate 2	replicate 3
Figure 2c													
B. theta	DMSO	0.16	0.16	0.00	0.66	0.39	0.66	14.79	14.73	11.85	29.18	27.70	26.58
	compound 7	0.26	0.24	0.00	0.63	0.17	0.00	1.55	0.96	0.87	0.33	0.00	0.20
	CAPE	0.42	0.72	0.52	0.64	0.28	0.16	5.36	2.32	2.31	2.06	0.90	0.81
B. fragilis	DMSO	100.00	100.00	100.00	100.00	100.00	100.00	99.00	99.38	99.50	99.05	99.39	99.31
	compound 7	1.14	1.51	1.11	4.96	4.15	2.69	10.78	9.04	6.33	9.74	8.92	5.67
	CAPE	88.33	85.35	84.93	98.64	98.42	99.12	98.65	99.13	98.66	98.95	98.93	99.13
B. vulgatus	DMSO	1.01	1.76	46.37	99.70	97.40	60.67	99.86	98.38	99.93	28.89	19.69	17.88
	compound 7	0.68	0.64	0.47	1.58	0.41	0.65	3.62	0.80	1.90	0.90	0.17	0.81
	CAPE	1.46	1.06	0.00	88.92	78.15	71.86	94.25	87.91	82.37	5.47	3.03	1.28
L. plantarum	DMSO	10.32	15.55	24.03	0.10	0.42	0.09	1.48	2.75	3.77	52.77	53.89	74.27
	compound 7	0.77	0.93	1.02	0.15	0.49	0.62	0.97	1.32	1.46	3.22	0.62	0.64
	CAPE	10.67	33.19	53.29	0.06	0.59	0.95	1.73	3.54	6.80	47.57	82.98	93.57
C. perfringens	DMSO	100.00	100.00	100.00	100.00	100.00	100.00	99.02	99.09	99.21	100.00	99.49	99.50
	compound 7	19.18	14.04	7.40	7.40	4.72	4.84	18.06	15.54	9.84	78.88	69.68	54.57
	CAPE	100.00	100.00	100.00	100.00	100.00	100.00	98.62	98.71	98.92	99.71	99.30	99.38
B. adolescentis	DMSO	100.00	100.00	100.00	87.65	87.58	88.64	100.00	99.37	99.16	100.00	99.79	99.45
	compound 7	2.88	3.09	2.93	0.34	0.37	0.73	1.26	1.21	1.54	10.43	6.05	7.35
	CAPE	100.00	100.00	100.00	100.00	100.00	100.00	99.43	100.00	99.43	99.85	100.00	99.71

Supplementary Table 3. Data collection and refinement statistics (molecular replacement)

	BSH	BSH-Compound
Data collection		
Space group	P 2_1 2_1 2_1	P 2_1 2_1 2
Cell dimensions		
a, *b*, *c* (Å)	84.88, 92.32, 194.25	98.58, 99.52, 162.12
α, β, γ (°)	90, 90, 90	90, 90, 90
Resolution (Å)	46.16 – 2.70 (2.80 – 2.70)*	47.57 – 3.50 (3.63 – 3.50)
R_{merge}	0.3686 (2.097)	0.1394 (1.989)
$I / \sigma I$	4.28 (0.93)	7.84 (0.86)
Completeness (%)	91.08 (92.25)	97.00 (95.32)
Redundancy	4.6 (4.6)	5.0 (5.2)
Refinement		
Resolution (Å)	46.16 – 2.70	47.57 – 3.50
No. reflections	38657	20032
R_{work} / R_{free}	0.2561 / 0.2982	0.2436 / 0.2932
No. atoms	10561	10249
Protein	10319	10221
Ligand/ion	-	28
Water	242	-
B-factors	34.45	187.80
Protein	34.56	187.69
Ligand/ion	-	230.31
Water	29.96	-
R.m.s. deviations		
Bond lengths (Å)	0.002	0.002
Bond angles (°)	0.51	0.46

*Highest-resolution shell is shown in parentheses. Each data set was collected using a single crystal.

Supplementary Table 4. In-gel digestion. Data correspond to Figure 4d and Supplementary Figure 15d. Average normalized spectral abundance factors (NSAF), average spectral counts, and average **7**-N_3 treated NSAF/control NSAF ratios for proteins detected from in-gel digestion of ~35 kDa bands from streptavidin pulldowns of clicked bacterial lysates. NSAFs were calculated according to reference 55 by normalizing to the total number of PSMs in each analysis. Averages were calculated across biological triplicates.

Protein Accessions	Av Control NSAF	Av Treated NSAF	Av Control Spectral Counts	Av Treated Spectral Counts	Av Treated NSAF/Control NSAF
tr|A7A5K1|A7A5K1_BIFAD	1.16E-01	5.24E-01	4.00	17.67	4.51

Supplementary Table 5. Bacterial Spectral Count Summary. Average normalized spectral abundance factors (NSAF), average spectral counts, and average **7**-N_3 treated NSAF/control NSAF ratios for proteins detected in streptavidin pulldowns of clicked bacterial lysates. NSAFs were calculated according to reference 55 and normalized to the total number of PSMs in each analysis. Averages were calculated across biological triplicates. Bacterial salt hydrolase is highlighted in red. Data were filtered for proteins with more than 5 spectral counts (averaged across biological triplicates) for **7**-N_3 treated samples. No proteins other than BSH were more than 2-fold enriched in probe-treated compared to control-treated samples.

Protein Accessions	Av Control NSAF	Av Treated NSAF	Av Control Spectral Counts	Av Treated Spectral Counts	Av Treated NSAF/Control NSAF
tr|A7A5K1|A7A5K1_BIFAD	1.26E-02	4.50E-02	2.00	10.00	3.58
tr|A7A833|A7A833_BIFAD	9.87E-03	1.50E-02	3.67	15.33	1.52
tr|A7A9D9|A7A9D9_BIFAD	9.12E-03	1.07E-02	3.00	6.00	1.18
tr|A7A4A2|A7A4A2_BIFAD	3.20E-02	3.26E-02	5.33	9.33	1.02
tr|A7A3U3|A7A3U3_BIFAD	1.32E-02	1.32E-02	4.00	7.00	1.00
tr|A7A595|A7A595_BIFAD	2.55E-02	2.13E-02	5.00	6.33	0.83
tr|A7A652|A7A652_BIFAD	1.81E-02	1.41E-02	7.00	10.00	0.78
tr|A7A662|A7A662_BIFAD	1.02E-02	7.77E-03	2.33	7.67	0.76
tr|A7A3U5|A7A3U5_BIFAD	2.95E-03	2.15E-03	4.00	9.33	0.73
tr|A7A425|A7A425_BIFAD	7.61E-02	5.44E-02	9.67	9.67	0.71
tr|A7A5N5|A7A5N5_BIFAD	1.99E-02	1.40E-02	3.33	6.00	0.71
tr|A7A4T1|A7A4T1_BIFAD	4.53E-02	2.74E-02	8.33	12.00	0.61
tr|A7A4M2|A7A4M2_BIFAD	2.76E-02	1.53E-02	5.00	7.33	0.55

Supplementary Table 6. Average normalized spectral abundance factors (NSAF), and average spectral counts for proteins reproducibly detected in streptavidin pulldowns of clicked bacterial lysates that were not **7**-N_3 treated (i.e. control pulldowns). NSAFs were calculated according to reference 55. Averages were calculated across biological triplicates.

Protein Accessions	Av Control NSAF	Av Control Spectral Counts
tr|A7A3I4|A7A3I4_BIFAD	7.31E-03	1.67
tr|A7A3X8|A7A3X8_BIFAD	2.50E-02	2.00
tr|A7A7V4|A7A7V4_BIFAD	6.69E-03	1.00
tr|A7A5M9|A7A5M9_BIFAD	9.41E-03	1.67
tr|A7A662|A7A662_BIFAD	1.02E-02	2.33
tr|A7A3I0|A7A3I0_BIFAD	1.13E-02	1.00
tr|A7A595|A7A595_BIFAD	2.55E-02	5.00
tr|A7A4T0|A7A4T0_BIFAD	1.12E-02	3.67
tr|A7A5N5|A7A5N5_BIFAD	1.99E-02	3.33
tr|A7A446|A7A446_BIFAD	2.19E-02	1.33
tr|A7A4T1|A7A4T1_BIFAD	4.53E-02	8.33
tr|A7A4M2|A7A4M2_BIFAD	2.76E-02	5.00
BSH ; tr|A7A5K1|A7A5K1_BIFAD	1.26E-02	2.00
tr|A7A9D9|A7A9D9_BIFAD	9.12E-03	3.00
tr|A7A425|A7A425_BIFAD	7.61E-02	9.67
tr|A7A3U5|A7A3U5_BIFAD	2.95E-03	4.00
tr|A7A428|A7A428_BIFAD	1.06E-02	1.33
tr|A7A4V3|A7A4V3_BIFAD	2.40E-02	1.00
tr|A7A4M1|A7A4M1_BIFAD	1.31E-02	2.00
tr|A7A641|A7A641_BIFAD	1.33E-02	1.33
tr|A7A652|A7A652_BIFAD	1.81E-02	7.00
tr|A7A423|A7A423_BIFAD	1.67E-02	1.67
tr|A7A8I7|A7A8I7_BIFAD	1.88E-02	3.00
tr|A7A833|A7A833_BIFAD	9.87E-03	3.67
tr|A7A792|A7A792_BIFAD	1.53E-02	1.00
tr|A7A3U3|A7A3U3_BIFAD	1.32E-02	4.00
tr|A7A429|A7A429_BIFAD	1.80E-02	1.00
tr|A7A445|A7A445_BIFAD	1.05E-01	2.00
tr|A7A3X9|A7A3X9_BIFAD	1.80E-02	1.00
tr|A7A3U9|A7A3U9_BIFAD	2.99E-02	1.33
tr|A7A436|A7A436_BIFAD	1.65E-02	1.00
tr|A7A4A2|A7A4A2_BIFAD	3.20E-02	5.33
tr|A7A3M7|A7A3M7_BIFAD	6.54E-02	2.00
tr|A7A422|A7A422_BIFAD	1.05E-02	1.00
tr|A7A9E7|A7A9E7_BIFAD	4.67E-03	1.00
tr|A7A8M6|A7A8M6_BIFAD	1.62E-02	2.33
tr|A7A5N6|A7A5N6_BIFAD	9.48E-03	3.00
tr|A7A4S8|A7A4S8_BIFAD	1.76E-02	1.00

Supplementary Table 7. Average normalized spectral abundance factors (NSAF), and average spectral counts for proteins reproducibly detected in streptavidin pulldowns of clicked bacterial **7**-N_3 treated lysates. NSAFs were calculated according to reference 55. Averages were calculated across biological triplicates.

Protein Accessions	Av Treated NSAF	Av Treated Spectral Counts
tr|A7A5Y9|A7A5Y9_BIFAD	1.36E-02	2.00
tr|A7A662|A7A662_BIFAD	7.77E-03	7.67
tr|A7A7V4|A7A7V4_BIFAD	5.49E-03	1.00
tr|A7A833|A7A833_BIFAD	1.50E-02	15.33
tr|A7A595|A7A595_BIFAD	2.13E-02	6.33
tr|A7A5N5|A7A5N5_BIFAD	1.40E-02	6.00
tr|A7A4T1|A7A4T1_BIFAD	2.74E-02	12.00
BSH ; tr|A7A5K1|A7A5K1_BIFAD	4.50E-02	10.00
tr|A7A3I0|A7A3I0_BIFAD	9.26E-03	1.00
tr|A7A9D9|A7A9D9_BIFAD	1.07E-02	6.00
tr|A7A425|A7A425_BIFAD	5.44E-02	9.67
tr|A7A428|A7A428_BIFAD	1.11E-02	5.00
tr|A7A4V3|A7A4V3_BIFAD	3.94E-02	2.00
tr|A7A4M1|A7A4M1_BIFAD	1.17E-02	4.00
tr|A7A641|A7A641_BIFAD	1.40E-02	2.00
tr|A7A652|A7A652_BIFAD	1.41E-02	10.00
tr|A7A445|A7A445_BIFAD	8.37E-02	2.67
tr|A7A436|A7A436_BIFAD	1.83E-02	3.00
tr|A7A8I7|A7A8I7_BIFAD	1.73E-02	5.00
tr|A7A4S8|A7A4S8_BIFAD	1.44E-02	1.00
tr|A7A3U3|A7A3U3_BIFAD	1.32E-02	7.00
tr|A7A423|A7A423_BIFAD	2.94E-02	4.33
tr|A7A3X9|A7A3X9_BIFAD	2.13E-02	1.67
tr|A7A4A2|A7A4A2_BIFAD	3.26E-02	9.33
tr|A7A3M7|A7A3M7_BIFAD	3.00E-02	1.67
tr|A7A3U5|A7A3U5_BIFAD	2.15E-03	9.33
tr|A7A5N6|A7A5N6_BIFAD	5.22E-03	5.00
tr|A7A4M2|A7A4M2_BIFAD	1.53E-02	7.33

Supplementary Figure 8. Average normalized spectral abundance factors (NSAF), average spectral counts, and average **7**-N_3 treated NSAF/control NSAF ratios for proteins detected in streptavidin pulldowns of clicked NCI-H716 lysates. NSAFs were calculated according to reference 55 and normalized to the total number of PSMs in each analysis. Averages were calculated across biological triplicates. Data were filtered for proteins with more than 5 spectral counts (averaged across biological triplicates) for 7-N3 treated samples. No proteins were more than 2-fold enriched in probe-treated compared to control-treated samples.

Protein Accessions	Av Control NSAF	Av Treated NSAF	Av Control Spectral Counts	Av Treated Spectral Counts	Av Treated NSAF/Control
sp|K22E_HUMAN|; sp|P35908|K22E_HUMAN	6.26E-03	9.97E-03	10.00	11.33	1.59
tr|A0A087X1W1|A0A087X1W1_HUMAN; tr|I3L182|I3L182_HUMAN; tr|I3L1C0|I3L1C0_HUMAN; tr|I3L1I8|I3L1I8_HUMAN; tr|I3L4D8|I3L4D8_HUMAN	8.05E-04	1.14E-03	5.33	7.00	1.42
sp|Q9UQ35|SRRM2_HUMAN	9.19E-03	1.12E-02	50.33	61.33	1.22
sp|P60709|ACTB_HUMAN; sp|P62736|ACTA_HUMAN; sp|P63261|ACTG_HUMAN; sp|P63267|ACTH_HUMAN; sp|P68032|ACTC_HUMAN; sp|P68133|ACTS_HUMAN; tr|A6NL76|A6NL76_HUMAN	3.83E-03	4.51E-03	7.00	5.67	1.18
sp|Q7L4I2|RSRC2_HUMAN	7.50E-03	6.28E-03	6.00	5.33	0.84
sp|P13639|EF2_HUMAN	3.10E-03	2.32E-03	19.33	7.67	0.75
sp|P06733|ENOA_HUMAN	4.80E-03	3.58E-03	10.00	5.67	0.75

Supplementary Table 9. Average normalized spectral abundance factors (NSAF), and average spectral counts for proteins reproducibly detected in streptavidin pulldowns of clicked NCI-H716 lysates that were not **7**-N_3 treated (i.e. control pulldowns). NSAFs were calculated according to reference 55. Averages were calculated across biological triplicates.

Protein Accessions	Av Control NSAF	Av Control Spectral Counts
sp|P04264|K2C1_HUMAN; sp|K22E_HUMAN|; sp|K2C1_HUMAN|; sp|P35908|K22E_HUMAN; sp|Q7Z794|K2C1B_HUMAN	7.82E-04	1.00
sp|Q9UQ35|SRRM2_HUMAN; tr|I3L0N7|I3L0N7_HUMAN; tr|I3L4D8|I3L4D8_HUMAN	7.05E-04	4.00
sp|Q5VTE0|EF1A3_HUMAN; sp|P68104|EF1A1_HUMAN; sp|Q05639|EF1A2_HUMAN; tr|A0A087WVQ9|A0A087WVQ9_HUMAN	2.01E-03	2.33
sp|Q13247|SRSF6_HUMAN	3.85E-03	2.67
sp|P47914|RL29_HUMAN	7.75E-03	3.33
gi|171455|gb|AAA88712.1|	2.84E-03	2.67
sp|P13647|K2C5_HUMAN; tr|F8VV57|F8VV57_HUMAN	1.30E-03	1.67
sp|Q59GN2|R39L5_HUMAN; sp|P62891|RL39_HUMAN	1.64E-02	2.00
sp|P04264|K2C1_HUMAN; sp|K2C1_HUMAN|	1.81E-02	25.00
tr|H0YHA7|H0YHA7_HUMAN; sp|Q07020|RL18_HUMAN; tr|A0A075B7A0|A0A075B7A0_HUMAN; tr|F8VYV2|F8VYV2_HUMAN; tr|G3V203|G3V203_HUMAN; tr|J3QQ67|J3QQ67_HUMAN	4.01E-03	1.67
sp|P60709|ACTB_HUMAN; sp|A5A3E0|POTEF_HUMAN; sp|P62736|ACTA_HUMAN; sp|P63261|ACTG_HUMAN; sp|P63267|ACTH_HUMAN; sp|P68032|ACTC_HUMAN; sp|P68133|ACTS_HUMAN; sp|Q6S8J3|POTEE_HUMAN; sp|Q9BYX7|ACTBM_HUMAN	2.83E-03	4.67
sp|Q9UQ35|SRRM2_HUMAN	9.19E-03	50.33
tr|E9PEB5|E9PEB5_HUMAN; sp|Q96AE4|FUBP1_HUMAN	7.50E-04	1.00
sp|Q5VTE0|EF1A3_HUMAN; sp|P68104|EF1A1_HUMAN; sp|Q05639|EF1A2_HUMAN; tr|A0A087WV01|A0A087WV01_HUMAN	1.07E-03	1.33
tr|H0YHA7|H0YHA7_HUMAN; sp|Q07020|RL18_HUMAN; tr|A0A075B7A0|A0A075B7A0_HUMAN; tr|F8VUA6|F8VUA6_HUMAN; tr|F8VYV2|F8VYV2_HUMAN; tr|G3V203|G3V203_HUMAN; tr|J3QQ67|J3QQ67_HUMAN	8.36E-03	3.00
sp|P60709|ACTB_HUMAN; sp|A5A3E0|POTEF_HUMAN; sp|P0CG38|POTEI_HUMAN; sp|P62736|ACTA_HUMAN; sp|P63261|ACTG_HUMAN; sp|P63267|ACTH_HUMAN; sp|P68032|ACTC_HUMAN; sp|P68133|ACTS_HUMAN; sp|Q6S8J3|POTEE_HUMAN; tr|A6NL76|A6NL76_HUMAN; tr|B8ZZJ2|B8ZZJ2_HUMAN; tr|C9JFL5|C9JFL5_HUMAN; tr|C9JTX5|C9JTX5_HUMAN; tr|C9JUM1|C9JUM1_HUMAN; tr|C9JZR7|C9JZR7_HUMAN; tr|E7EVS6|E7EVS6_HUMAN; tr|F6QUT6|F6QUT6_HUMAN; tr|F6UVQ4|F6UVQ4_HUMAN; tr|F8WB63|F8WB63_HUMAN; tr|F8WCH0|F8WCH0_HUMAN; tr|G5E9R0|G5E9R0_HUMAN; tr|I3L1U9|I3L1U9_HUMAN; tr|I3L3I0|I3L3I0_HUMAN; tr|I3L3R2|I3L3R2_HUMAN; tr|I3L4N8|I3L4N8_HUMAN; tr|J3KT65|J3KT65_HUMAN; tr|K7EM38|K7EM38_HUMAN	2.70E-03	3.33
sp|P07437|TBB5_HUMAN; tr|Q5JP53|Q5JP53_HUMAN	1.13E-03	1.67
sp|Q9UQ35|SRRM2_HUMAN; tr|A0A087X1W1|A0A087X1W1_HUMAN; tr|I3L182|I3L182_HUMAN; tr|I3L1C0|I3L1C0_HUMAN; tr|I3L1I8|I3L1I8_HUMAN; tr|I3L4D8|I3L4D8_HUMAN	8.05E-04	5.33
tr|E7ENU7|E7ENU7_HUMAN; sp|P61313|RL15_HUMAN; tr|E7EQV9|E7EQV9_HUMAN; tr|E7EX53|E7EX53_HUMAN	2.64E-03	1.33
sp|Q9Y383|LC7L2_HUMAN; sp|Q9NQ29|LUC7L_HUMAN; tr|A0A0A6YYJ8|A0A0A6YYJ8_HUMAN; tr|A8MYV2|A8MYV2_HUMAN; tr|B8ZZ10|B8ZZ10_HUMAN	1.10E-03	1.00

sp|Q9UQ35|SRRM2_HUMAN; tr|I3L182|I3L182_HUMAN; tr|I3L1I8|I3L1I8_HUMAN; tr|I3L4D8|I3L4D8_HUMAN	4.28E-04	2.67
sp|Q02878|RL6_HUMAN	2.26E-03	1.33
tr|Q5T760|Q5T760_HUMAN; sp|Q05519|SRS11_HUMAN	1.22E-03	1.00
sp|P08238|HS90B_HUMAN; sp|Q58FF8|H90B2_HUMAN	6.20E-04	1.00
tr|E9PR30|E9PR30_HUMAN; sp|P62861|RS30_HUMAN	4.75E-03	1.00
tr|J3KPP4|J3KPP4_HUMAN; sp|O95232|LC7L3_HUMAN; tr|D6RDI2|D6RDI2_HUMAN	1.72E-03	1.67
sp|P06733|ENOA_HUMAN; tr|K7EM90|K7EM90_HUMAN	3.03E-03	7.33
tr|G3V1A1|G3V1A1_HUMAN; sp|P62917|RL8_HUMAN; tr|E9PKZ0|E9PKZ0_HUMAN	4.45E-03	2.33
tr|H0YDJ3|H0YDJ3_HUMAN; sp|Q13523|PRP4B_HUMAN	3.76E-03	4.33
sp|P08621|RU17_HUMAN; tr|M0QYR1|M0QYR1_HUMAN	6.41E-03	6.00
sp|P07437|TBB5_HUMAN; sp|Q13509|TBB3_HUMAN; sp|Q13885|TBB2A_HUMAN; sp|Q9BVA1|TBB2B_HUMAN; tr|A0A0B4J269|A0A0B4J269_HUMAN; tr|G3V2N6|G3V2N6_HUMAN; tr|G3V2R8|G3V2R8_HUMAN; tr|G3V3R4|G3V3R4_HUMAN; tr|G3V5W4|G3V5W4_HUMAN; tr|Q5JP53|Q5JP53_HUMAN	3.01E-03	5.67
sp|P07900|HS90A_HUMAN	1.11E-03	6.67
sp|P06733|ENOA_HUMAN	4.80E-03	10.00
sp|P62937|PPIA_HUMAN	5.45E-03	7.33
sp|P13647|K2C5_HUMAN; tr|F8W0C6|F8W0C6_HUMAN; tr|H0YIN9|H0YIN9_HUMAN	1.73E-03	2.00
tr|Q5T760|Q5T760_HUMAN; sp|Q05519|SRS11_HUMAN; tr|B4DWT1|B4DWT1_HUMAN	6.80E-03	5.67
tr|E9PLL6|E9PLL6_HUMAN; sp|P46776|RL27A_HUMAN	6.63E-03	1.67
sp|P10809|CH60_HUMAN	2.56E-03	7.00
sp|Q9H7N4|SFR19_HUMAN	5.81E-04	1.67
sp|Q9UQ35|SRRM2_HUMAN; tr|I3L4D8|I3L4D8_HUMAN	3.45E-04	2.00
sp|P62805|H4_HUMAN	4.56E-03	1.00
sp|P08621|RU17_HUMAN	4.11E-03	4.67
sp|P60709|ACTB_HUMAN; sp|P62736|ACTA_HUMAN; sp|P63261|ACTG_HUMAN; sp|P63267|ACTH_HUMAN; sp|P68032|ACTC_HUMAN; sp|P68133|ACTS_HUMAN; tr|A6NL76|A6NL76_HUMAN	3.83E-03	7.00
sp|P13639|EF2_HUMAN	3.10E-03	19.33
tr|U3KQK0|U3KQK0_HUMAN; sp|O60814|H2B1K_HUMAN; sp|P06899|H2B1J_HUMAN; sp|P23527|H2B1O_HUMAN; sp|P33778|H2B1B_HUMAN; sp|P57053|H2BFS_HUMAN; sp|P58876|H2B1D_HUMAN; sp|P62807|H2B1C_HUMAN; sp|Q16778|H2B2E_HUMAN; sp|Q5QNW6|H2B2F_HUMAN; sp|Q8N257|H2B3B_HUMAN; sp|Q93079|H2B1H_HUMAN; sp|Q96A08|H2B1A_HUMAN; sp|Q99877|H2B1N_HUMAN; sp|Q99879|H2B1M_HUMAN; sp|Q99880|H2B1L_HUMAN	2.89E-03	1.33
sp|P00558|PGK1_HUMAN; sp|P07205|PGK2_HUMAN	1.43E-03	2.67
tr|G3V1A4|G3V1A4_HUMAN; sp|P23528|COF1_HUMAN; sp|Q9Y281|COF2_HUMAN; tr|E9PK25|E9PK25_HUMAN; tr|E9PLJ3|E9PLJ3_HUMAN; tr|E9PP50|E9PP50_HUMAN; tr|E9PQB7|E9PQB7_HUMAN	3.19E-03	1.33
sp|P12277|KCRB_HUMAN; tr|G3V461|G3V461_HUMAN; tr|G3V4N7|G3V4N7_HUMAN	1.67E-03	3.67
sp|P08779|K1C16_HUMAN	1.96E-03	1.67
sp|P60174|TPIS_HUMAN	3.19E-03	4.67
sp|P31942|HNRH3_HUMAN	1.47E-03	1.33
sp|K22E_HUMAN|; sp|P35908|K22E_HUMAN	6.26E-03	10.00
sp|Q5T749|KPRP_HUMAN	8.45E-04	1.67
sp|P00558|PGK1_HUMAN	3.54E-03	10.00

sp|Q9UQ35|SRRM2_HUMAN; tr|I3L182|I3L182_HUMAN; tr|I3L1I8|I3L1I8_HUMAN; tr|I3L4D8|I3L4D8_HUMAN	4.28E-04	2.67
sp|Q02878|RL6_HUMAN	2.26E-03	1.33
tr|Q5T760|Q5T760_HUMAN; sp|Q05519|SRS11_HUMAN	1.22E-03	1.00
sp|P08238|HS90B_HUMAN; sp|Q58FF8|H90B2_HUMAN	6.20E-04	1.00
tr|E9PR30|E9PR30_HUMAN; sp|P62861|RS30_HUMAN	4.75E-03	1.00
tr|J3KPP4|J3KPP4_HUMAN; sp|O95232|LC7L3_HUMAN; tr|D6RDI2|D6RDI2_HUMAN	1.72E-03	1.67
sp|P06733|ENOA_HUMAN; tr|K7EM90|K7EM90_HUMAN	3.03E-03	7.33
tr|G3V1A1|G3V1A1_HUMAN; sp|P62917|RL8_HUMAN; tr|E9PKZ0|E9PKZ0_HUMAN	4.45E-03	2.33
tr|H0YDJ3|H0YDJ3_HUMAN; sp|Q13523|PRP4B_HUMAN	3.76E-03	4.33
sp|P08621|RU17_HUMAN; tr|M0QYR1|M0QYR1_HUMAN	6.41E-03	6.00
sp|P07437|TBB5_HUMAN; sp|Q13509|TBB3_HUMAN; sp|Q13885|TBB2A_HUMAN; sp|Q9BVA1|TBB2B_HUMAN; tr|A0A0B4J269|A0A0B4J269_HUMAN; tr|G3V2N6|G3V2N6_HUMAN; tr|G3V2R8|G3V2R8_HUMAN; tr|G3V3R4|G3V3R4_HUMAN; tr|G3V5W4|G3V5W4_HUMAN; tr|Q5JP53|Q5JP53_HUMAN	3.01E-03	5.67
sp|P07900|HS90A_HUMAN	1.11E-03	6.67
sp|P06733|ENOA_HUMAN	4.80E-03	10.00
sp|P62937|PPIA_HUMAN	5.45E-03	7.33
sp|P13647|K2C5_HUMAN; tr|F8W0C6|F8W0C6_HUMAN; tr|H0YIN9|H0YIN9_HUMAN	1.73E-03	2.00
tr|Q5T760|Q5T760_HUMAN; sp|Q05519|SRS11_HUMAN; tr|B4DWT1|B4DWT1_HUMAN	6.80E-03	5.67
tr|E9PLL6|E9PLL6_HUMAN; sp|P46776|RL27A_HUMAN	6.63E-03	1.67
sp|P10809|CH60_HUMAN	2.56E-03	7.00
sp|Q9H7N4|SFR19_HUMAN	5.81E-04	1.67
sp|Q9UQ35|SRRM2_HUMAN; tr|I3L4D8|I3L4D8_HUMAN	3.45E-04	2.00
sp|P62805|H4_HUMAN	4.56E-03	1.00
sp|P08621|RU17_HUMAN	4.11E-03	4.67
sp|P60709|ACTB_HUMAN; sp|P62736|ACTA_HUMAN; sp|P63261|ACTG_HUMAN; sp|P63267|ACTH_HUMAN; sp|P68032|ACTC_HUMAN; sp|P68133|ACTS_HUMAN; tr|A6NL76|A6NL76_HUMAN	3.83E-03	7.00
sp|P13639|EF2_HUMAN	3.10E-03	19.33
tr|U3KQK0|U3KQK0_HUMAN; sp|O60814|H2B1K_HUMAN; sp|P06899|H2B1J_HUMAN; sp|P23527|H2B1O_HUMAN; sp|P33778|H2B1B_HUMAN; sp|P57053|H2BFS_HUMAN; sp|P58876|H2B1D_HUMAN; sp|P62807|H2B1C_HUMAN; sp|Q16778|H2B2E_HUMAN; sp|Q5QNW6|H2B2F_HUMAN; sp|Q8N257|H2B3B_HUMAN; sp|Q93079|H2B1H_HUMAN; sp|Q96A08|H2B1A_HUMAN; sp|Q99877|H2B1N_HUMAN; sp|Q99879|H2B1M_HUMAN; sp|Q99880|H2B1L_HUMAN	2.89E-03	1.33
sp|P00558|PGK1_HUMAN; sp|P07205|PGK2_HUMAN	1.43E-03	2.67
tr|G3V1A4|G3V1A4_HUMAN; sp|P23528|COF1_HUMAN; sp|Q9Y281|COF2_HUMAN; tr|E9PK25|E9PK25_HUMAN; tr|E9PLJ3|E9PLJ3_HUMAN; tr|E9PP50|E9PP50_HUMAN; tr|E9PQB7|E9PQB7_HUMAN	3.19E-03	1.33
sp|P12277|KCRB_HUMAN; tr|G3V461|G3V461_HUMAN; tr|G3V4N7|G3V4N7_HUMAN	1.67E-03	3.67
sp|P08779|K1C16_HUMAN	1.96E-03	1.67
sp|P60174|TPIS_HUMAN	3.19E-03	4.67
sp|P31942|HNRH3_HUMAN	1.47E-03	1.33
sp|K22E_HUMAN|; sp|P35908|K22E_HUMAN	6.26E-03	10.00
sp|Q5T749|KPRP_HUMAN	8.45E-04	1.67
sp|P00558|PGK1_HUMAN	3.54E-03	10.00

Supplementary Table 10. Average normalized spectral abundance factors (NSAF), and average spectral counts for proteins reproducibly detected in streptavidin pulldowns of clicked NCI-H716 lysates. NSAFs were calculated according to reference 55. Averages were calculated across biological triplicates.

Protein Accessions	Av Treated NSAF	Av Treated Spectral Counts
sp|P60709|ACTB_HUMAN; sp|P63261|ACTG_HUMAN; tr|E7EVS6|E7EVS6_HUMAN; tr|G5E9R0|G5E9R0_HUMAN; tr|I3L1U9|I3L1U9_HUMAN; tr|I3L3I0|I3L3I0_HUMAN; tr|I3L3R2|I3L3R2_HUMAN; tr|I3L4N8|I3L4N8_HUMAN; tr|J3KT65|J3KT65_HUMAN; tr|K7EM38|K7EM38_HUMAN	3.12E-03	3.33
tr|J3QT28|J3QT28_HUMAN; sp|O43684|BUB3_HUMAN	1.70E-03	1.00
tr|A0A087WW55|A0A087WW55_HUMAN; sp|P07477|TRY1_HUMAN; sp|P07478|TRY2_HUMAN; sp|Q8NHM4|TRY6_HUMAN; tr|A0A0J9YYC8|A0A0J9YYC8_HUMAN; tr|A6XMV8|A6XMV8_HUMAN; tr|A6XMV9|A6XMV9_HUMAN; tr|E7EQ64|E7EQ64_HUMAN; tr|H0Y8D1|H0Y8D1_HUMAN	2.89E-03	1.33
sp|Q9UQ35|SRRM2_HUMAN; tr|I3L0N7|I3L0N7_HUMAN; tr|I3L4D8|I3L4D8_HUMAN	8.30E-04	4.67
sp|Q9UQ35|SRRM2_HUMAN; tr|I3L182|I3L182_HUMAN; tr|I3L1I8|I3L1I8_HUMAN; tr|I3L4D8|I3L4D8_HUMAN	6.26E-04	3.33
sp|Q9UQ35|SRRM2_HUMAN; tr|I3L3Q8|I3L3Q8_HUMAN	5.46E-04	3.00
tr|U3KQK0|U3KQK0_HUMAN; sp|O60814|H2B1K_HUMAN; sp|P06899|H2B1J_HUMAN; sp|P23527|H2B1O_HUMAN; sp|P33778|H2B1B_HUMAN; sp|P57053|H2BFS_HUMAN; sp|P58876|H2B1D_HUMAN; sp|P62807|H2B1C_HUMAN; sp|Q16778|H2B2E_HUMAN; sp|Q5QNW6|H2B2F_HUMAN; sp|Q8N257|H2B3B_HUMAN; sp|Q93079|H2B1H_HUMAN; sp|Q96A08|H2B1A_HUMAN; sp|Q99877|H2B1N_HUMAN; sp|Q99879|H2B1M_HUMAN; sp|Q99880|H2B1L_HUMAN	2.91E-03	1.00
tr|J3KTE4|J3KTE4_HUMAN; sp|P84098|RL19_HUMAN; tr|J3QL15|J3QL15_HUMAN; tr|J3QR09|J3QR09_HUMAN	2.34E-03	1.00
sp|Q9UQ35|SRRM2_HUMAN; tr|A0A087X1W1|A0A087X1W1_HUMAN; tr|I3L182|I3L182_HUMAN; tr|I3L1I8|I3L1I8_HUMAN; tr|I3L4D8|I3L4D8_HUMAN	1.82E-04	1.00
tr|H0YHA7|H0YHA7_HUMAN; sp|Q07020|RL18_HUMAN; tr|F8VUA6|F8VUA6_HUMAN; tr|G3V203|G3V203_HUMAN; tr|J3QQ67|J3QQ67_HUMAN	1.14E-02	4.00
sp|Q5VTL8|PR38B_HUMAN; tr|A0A0A0MRN0|A0A0A0MRN0_HUMAN	1.22E-03	1.33
sp|P08238|HS90B_HUMAN; sp|Q58FF8|H90B2_HUMAN	6.53E-04	1.00
sp|Q13247|SRSF6_HUMAN	2.29E-03	2.00
sp|TRYP_PIG|	1.54E-01	65.00
sp|O75400|PR40A_HUMAN	9.51E-04	1.67
tr|E9PR30|E9PR30_HUMAN; sp|P62861|RS30_HUMAN	5.01E-03	1.00
sp|Q8WUQ7|CATIN_HUMAN	6.15E-04	1.00
tr|A0A0C4DG89|A0A0C4DG89_HUMAN; sp|Q7L014|DDX46_HUMAN	1.65E-03	3.67
sp|Q9Y383|LC7L2_HUMAN; tr|F8WEU3|F8WEU3_HUMAN; tr|V9GZ75|V9GZ75_HUMAN	1.28E-03	1.33
tr|G3V1A1|G3V1A1_HUMAN; sp|P62917|RL8_HUMAN; tr|E9PKZ0|E9PKZ0_HUMAN	3.28E-03	1.33

gi|171455|gb|AAA88712.1|	3.40E-03	2.67
tr|A0A0U1RQH7|A0A0U1RQH7_HUMAN; sp|Q14498|RBM39_HUMAN; tr|G3XAC6|G3XAC6_HUMAN; tr|H0Y4X3|H0Y4X3_HUMAN; tr|Q5QP23|Q5QP23_HUMAN	3.17E-03	1.67
sp|P60709|ACTB_HUMAN; sp|P63261|ACTG_HUMAN	2.86E-03	2.67
tr|J3KPP4|J3KPP4_HUMAN; sp|O95232|LC7L3_HUMAN; tr|D6RDI2|D6RDI2_HUMAN	1.77E-03	1.67
sp|P12277|KCRB_HUMAN; tr|G3V461|G3V461_HUMAN; tr|G3V4N7|G3V4N7_HUMAN	1.79E-03	2.33
sp|Q59GN2|R39L5_HUMAN; sp|P62891|RL39_HUMAN	9.52E-03	1.33
sp|P06733|ENOA_HUMAN; tr|K7EM90|K7EM90_HUMAN	2.61E-03	4.00
sp|P13639|EF2_HUMAN	2.32E-03	7.67
sp|LYSC_CHICK|	6.52E-03	2.00
sp|P60174|TPIS_HUMAN	2.47E-03	2.33
sp|P00558|PGK1_HUMAN; sp|P07205|PGK2_HUMAN	2.36E-03	3.00
sp|P47914|RL29_HUMAN	6.14E-03	2.00
sp|Q5JTW2|CEP78_HUMAN; tr|A8MST6|A8MST6_HUMAN	7.07E-04	1.00
tr|A0A0B4J1Z1|A0A0B4J1Z1_HUMAN; sp|Q16629|SRSF7_HUMAN; tr|C9JAB2|C9JAB2_HUMAN	8.33E-03	2.33
sp|P08621|RU17_HUMAN; tr|M0QYR1|M0QYR1_HUMAN	3.66E-03	3.33
sp|Q7L4I2|RSRC2_HUMAN	6.28E-03	5.33
sp|Q9UQ35|SRRM2_HUMAN; tr|I3L182|I3L182_HUMAN; tr|I3L4D8|I3L4D8_HUMAN	2.62E-04	1.33
tr|H0YHA7|H0YHA7_HUMAN; sp|Q07020|RL18_HUMAN; tr|A0A075B7A0|A0A075B7A0_HUMAN; tr|F8VYV2|F8VYV2_HUMAN; tr|G3V203|G3V203_HUMAN; tr|J3QQ67|J3QQ67_HUMAN	5.42E-03	1.67
sp|P60709|ACTB_HUMAN; sp|A5A3E0|POTEF_HUMAN; sp|P62736|ACTA_HUMAN; sp|P63261|ACTG_HUMAN; sp|P63267|ACTH_HUMAN; sp|P68032|ACTC_HUMAN; sp|P68133|ACTS_HUMAN; sp|Q6S8J3|POTEE_HUMAN; sp|Q9BYX7|ACTBM_HUMAN	1.96E-03	2.67
sp|P60709|ACTB_HUMAN; sp|P62736|ACTA_HUMAN; sp|P63261|ACTG_HUMAN; sp|P63267|ACTH_HUMAN; sp|P68032|ACTC_HUMAN; sp|P68133|ACTS_HUMAN; tr|A6NL76|A6NL76_HUMAN	4.51E-03	5.67
sp|P10768|ESTD_HUMAN	1.71E-03	1.00
sp|Q5T749|KPRP_HUMAN	1.88E-03	2.00
sp|Q9UQ35|SRRM2_HUMAN	1.12E-02	61.33
sp|P07900|HS90A_HUMAN	1.10E-03	3.33
sp|K22E_HUMAN|; sp|P35908|K22E_HUMAN	9.97E-03	11.33
sp|P06733|ENOA_HUMAN	3.58E-03	5.67
tr|A0A087WZ27|A0A087WZ27_HUMAN; sp|P62249|RS16_HUMAN; tr|M0QX76|M0QX76_HUMAN; tr|M0R1M5|M0R1M5_HUMAN; tr|M0R210|M0R210_HUMAN; tr|M0R3H0|M0R3H0_HUMAN; tr|Q6IPX4|Q6IPX4_HUMAN	4.13E-03	1.33
tr|H0YDJ3|H0YDJ3_HUMAN; sp|Q13523|PRP4B_HUMAN	2.68E-03	3.00
sp|P22626|ROA2_HUMAN	4.32E-03	4.00
tr|H0YHA7|H0YHA7_HUMAN; sp|Q07020|RL18_HUMAN; tr|A0A075B7A0|A0A075B7A0_HUMAN; tr|F8VUA6|F8VUA6_HUMAN; tr|F8VYV2|F8VYV2_HUMAN; tr|G3V203|G3V203_HUMAN; tr|J3QQ67|J3QQ67_HUMAN	1.09E-02	3.33

tr|K7EJT5|K7EJT5_HUMAN; sp|P35268|RL22_HUMAN; tr|K7EKS7|K7EKS7_HUMAN; tr|K7ELC4|K7ELC4_HUMAN; tr|K7EMH1|K7EMH1_HUMAN; tr|K7EP65|K7EP65_HUMAN; tr|K7ERI7|K7ERI7_HUMAN	1.07E-02	1.00
tr|Q5T760|Q5T760_HUMAN; sp|Q05519|SRS11_HUMAN; tr|B4DWT1|B4DWT1_HUMAN	6.10E-03	4.00
tr|A0A0C4DG62|A0A0C4DG62_HUMAN; sp|Q66PJ3|AR6P4_HUMAN; tr|A0A0C4DH18|A0A0C4DH18_HUMAN; tr|F5GYV5|F5GYV5_HUMAN; tr|F8WCT1|F8WCT1_HUMAN; tr|F8WEP2|F8WEP2_HUMAN; tr|H7BZV4|H7BZV4_HUMAN	2.21E-03	1.00
tr|A0A0C4DG89|A0A0C4DG89_HUMAN; sp|Q7L014|DDX46_HUMAN; tr|D6RJA6|D6RJA6_HUMAN	1.77E-03	3.33
sp|P10809|CH60_HUMAN; tr|C9JL25|C9JL25_HUMAN; tr|E7ESH4|E7ESH4_HUMAN; tr|E7EXB4|E7EXB4_HUMAN	1.28E-03	1.33
tr|A0A087WWP4|A0A087WWP4_HUMAN; sp|Q96T37|RBM15_HUMAN	5.34E-04	1.00
sp|P60709|ACTB_HUMAN; sp|A5A3E0|POTEF_HUMAN; sp|P0CG38|POTEI_HUMAN; sp|P62736|ACTA_HUMAN; sp|P63261|ACTG_HUMAN; sp|P63267|ACTH_HUMAN; sp|P68032|ACTC_HUMAN; sp|P68133|ACTS_HUMAN; sp|Q6S8J3|POTEE_HUMAN; tr|A6NL76|A6NL76_HUMAN; tr|B8ZZJ2|B8ZZJ2_HUMAN; tr|C9JFL5|C9JFL5_HUMAN; tr|C9JTX5|C9JTX5_HUMAN; tr|C9JUM1|C9JUM1_HUMAN; tr|C9JZR7|C9JZR7_HUMAN; tr|E7EVS6|E7EVS6_HUMAN; tr|F6QUT6|F6QUT6_HUMAN; tr|F6UVQ4|F6UVQ4_HUMAN; tr|F8WB63|F8WB63_HUMAN; tr|F8WCH0|F8WCH0_HUMAN; tr|G5E9R0|G5E9R0_HUMAN; tr|I3L1U9|I3L1U9_HUMAN; tr|I3L3I0|I3L3I0_HUMAN; tr|I3L3R2|I3L3R2_HUMAN; tr|I3L4N8|I3L4N8_HUMAN; tr|J3KT65|J3KT65_HUMAN; tr|K7EM38|K7EM38_HUMAN	1.83E-03	2.33
sp|P10809|CH60_HUMAN	1.53E-03	3.33
sp|P04259|K2C6B_HUMAN; sp|P02538|K2C6A_HUMAN; sp|P48668|K2C6C_HUMAN	3.19E-03	3.67
tr|D3YTB1|D3YTB1_HUMAN; sp|P62910|RL32_HUMAN; tr|F8W727|F8W727_HUMAN	1.52E-02	4.00
tr|E7ENU7|E7ENU7_HUMAN; sp|P61313|RL15_HUMAN; tr|E7EQV9|E7EQV9_HUMAN	3.87E-03	1.33
sp|Q5T200|ZC3HD_HUMAN	3.05E-04	1.33
sp|Q9UQ35|SRRM2_HUMAN; tr|A0A087X1W1|A0A087X1W1_HUMAN; tr|I3L182|I3L182_HUMAN; tr|I3L1C0|I3L1C0_HUMAN; tr|I3L1I8|I3L1I8_HUMAN; tr|I3L4D8|I3L4D8_HUMAN	1.14E-03	7.00
sp|Q9H7N4|SFR19_HUMAN	1.09E-03	2.33
sp|Q9UQ35|SRRM2_HUMAN; tr|I3L4D8|I3L4D8_HUMAN	4.47E-04	2.33
sp|P62805|H4_HUMAN	4.81E-03	1.00
tr|M0R0P7|M0R0P7_HUMAN; sp|Q02543|RL18A_HUMAN; tr|M0R117|M0R117_HUMAN; tr|M0R1A7|M0R1A7_HUMAN; tr|M0R3D6|M0R3D6_HUMAN	4.70E-03	2.33
tr|J3KQE5|J3KQE5_HUMAN; sp|P62826|RAN_HUMAN; tr|B4DV51|B4DV51_HUMAN; tr|B5MDF5|B5MDF5_HUMAN; tr|F5H018|F5H018_HUMAN	2.43E-03	1.67
tr|E7EUT5|E7EUT5_HUMAN; sp|P04406|G3P_HUMAN	3.44E-03	2.33
tr|J3KPP4|J3KPP4_HUMAN; sp|O95232|LC7L3_HUMAN	9.30E-04	1.00
sp|P08621|RU17_HUMAN	4.04E-03	3.33

tr|B5MC07|B5MC07_HUMAN; sp|O95994|AGR2_HUMAN; sp|Q8TD06|AGR3_HUMAN; tr|B5MC62|B5MC62_HUMAN; tr|H7C040|H7C040_HUMAN; tr|H7C3Z9|H7C3Z9_HUMAN	7.12E-03	3.67
tr|Q5T760|Q5T760_HUMAN; sp|Q05519|SRS11_HUMAN; tr|B4DWT1|B4DWT1_HUMAN; tr|S4R3C4|S4R3C4_HUMAN	1.29E-03	1.00
tr|A0A0U1RQH7|A0A0U1RQH7_HUMAN; sp|Q14498|RBM39_HUMAN; tr|G3XAC6|G3XAC6_HUMAN; tr|H0Y4X3|H0Y4X3_HUMAN; tr|Q5QP22|Q5QP22_HUMAN; tr|Q5QP23|Q5QP23_HUMAN	2.03E-03	1.00
sp|P12277|KCRB_HUMAN; tr|H0YJG0|H0YJG0_HUMAN	3.22E-03	3.67
tr|Q5T760|Q5T760_HUMAN; sp|Q05519|SRS11_HUMAN; tr|Q5T757|Q5T757_HUMAN	2.60E-03	2.00

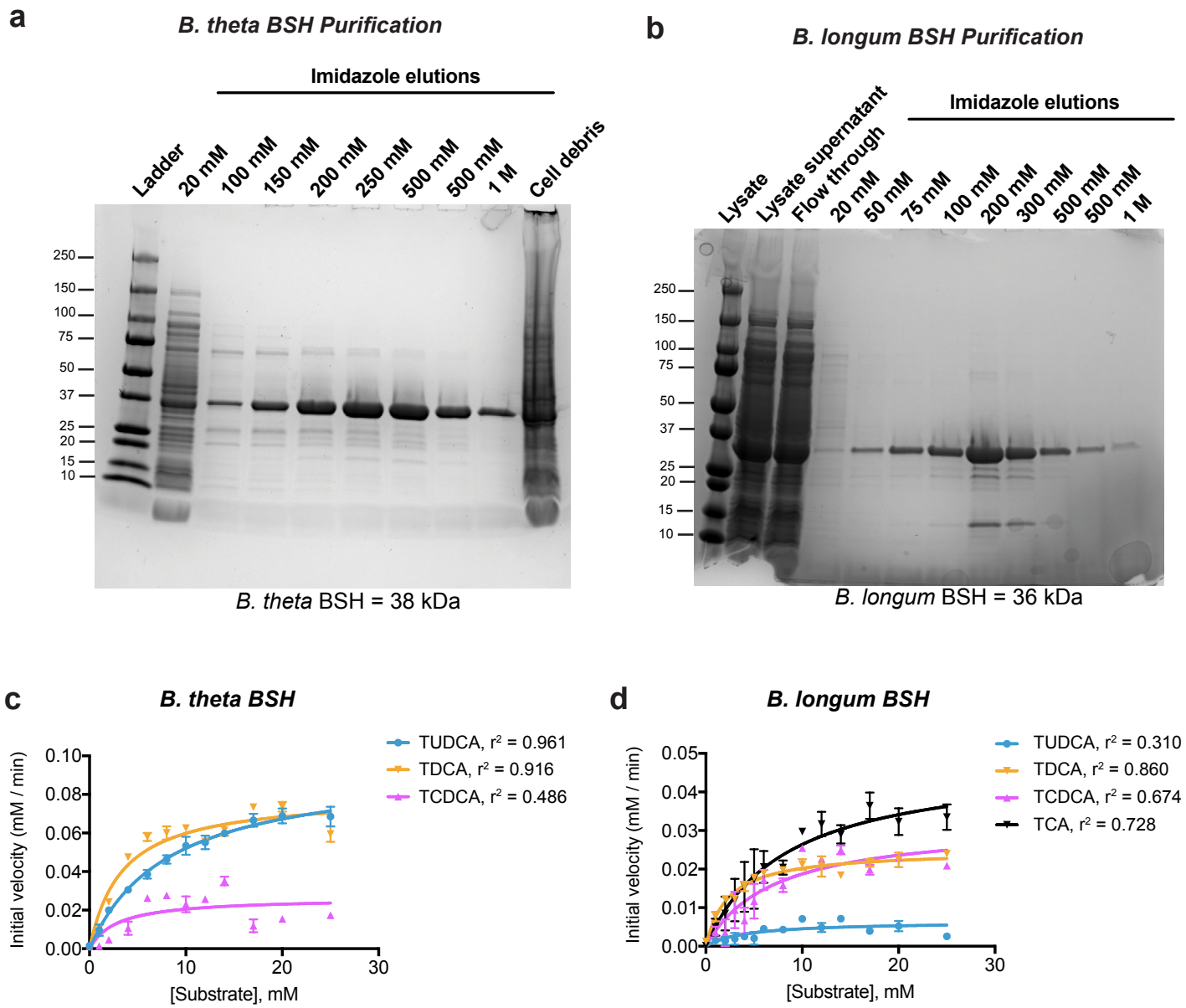

Supplementary Figure 1. Purification and kinetic characterization of BSHs. (**a**) SDS-PAGE of *B. theta* BSH purification. Experiment was repeated seven times with similar results. (**b**) SDS-PAGE of *B. longum* BSH purification. Experiment was repeated four time with similar results. (**c**-**d**) Michaelis-Menten analysis of BSH kinetic data. Rate vs substrate concentration curves for *B. theta* BSH (**c**) and *B. longum* BSH (**d**). Each data point for both was obtained under initial velocity conditions in which less than 10% starting material was consumed. Assays were performed in biological triplicate, and all data are presented as mean ± SEM. Curves were fit using non-linear regression analysis (Michaelis-Menten) in Graphpad Prism using the default parameters. Note: previously reported BSH kinetic parameters have been determined at the optimal pH of the enzymes (pH 4.2-6.5). We observed similar pH-dependent behavior for deconjugation by *B. theta* BSH and *B. longum* BSH. As a result, because all kinetic experiments herein were performed at physiological pH (7.5), lower kcat values were obtained for these two enzymes than typical literature values for similar enzymes.

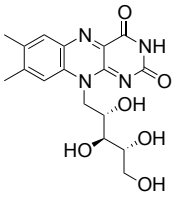

Riboflavin (**10**)

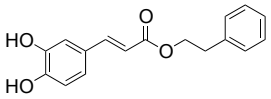

Caffeic acid phenethyl ester
(CAPE, **11**)

Supplementary Figure 2. Structures of the BSH inhibitors riboflavin (10) and caffeic acid phenethyl ester (CAPE, 11) previously discovered through a high-throughput screen.

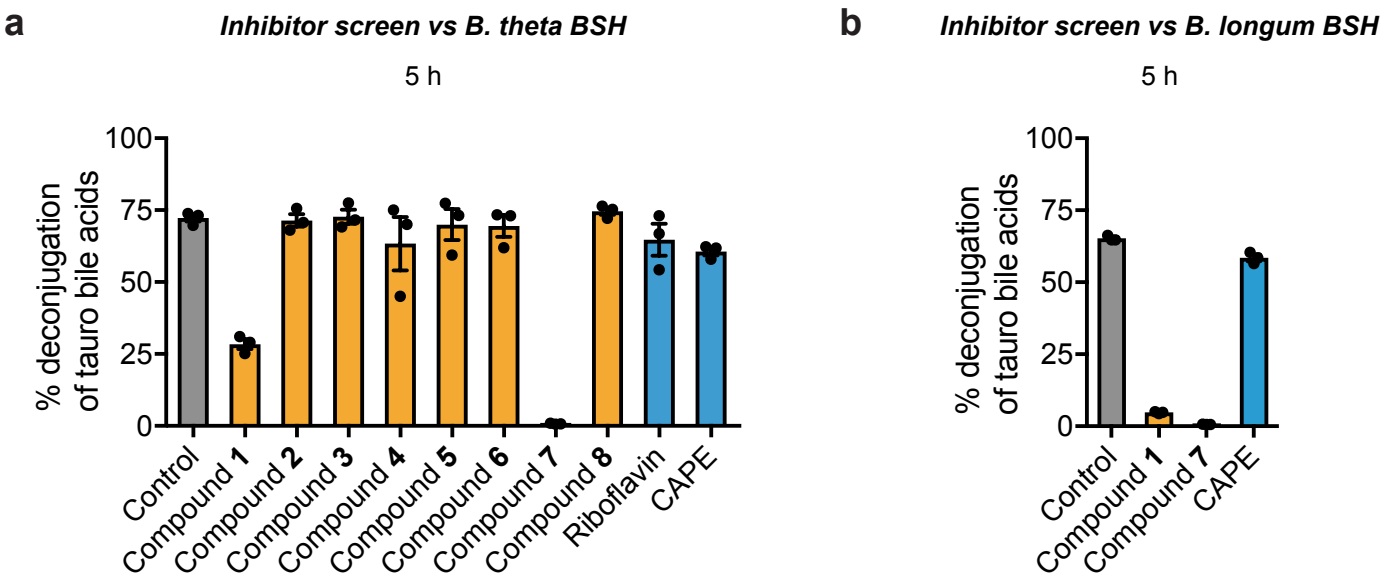

Supplementary Figure 3. Identification of compound 7 as a potent broad-spectrum BSH inhibitor. (**a**,**b**) Screen of inhibitors versus *B. theta* BSH (**a**) and B. longum BSH (**b**) showing % deconjugation of tauro bile acids at 5 hours. Inhibitor (100 μM) was incubated with 200 nM rBSH for 30 mins followed by addition of taurine-conjugated bile acid substrates (tauro-β-muricholic acid, TβMCA; tauro-cholic acid, TCA; tauro-ursodeoxycholic acid, TUDCA; and tauro-deoxycholic acid, TDCA, 25 μM each). Deconjugation of substrate was followed by UPLC-MS. Assays were performed in biological triplicate, and all data are presented as mean ± SEM.

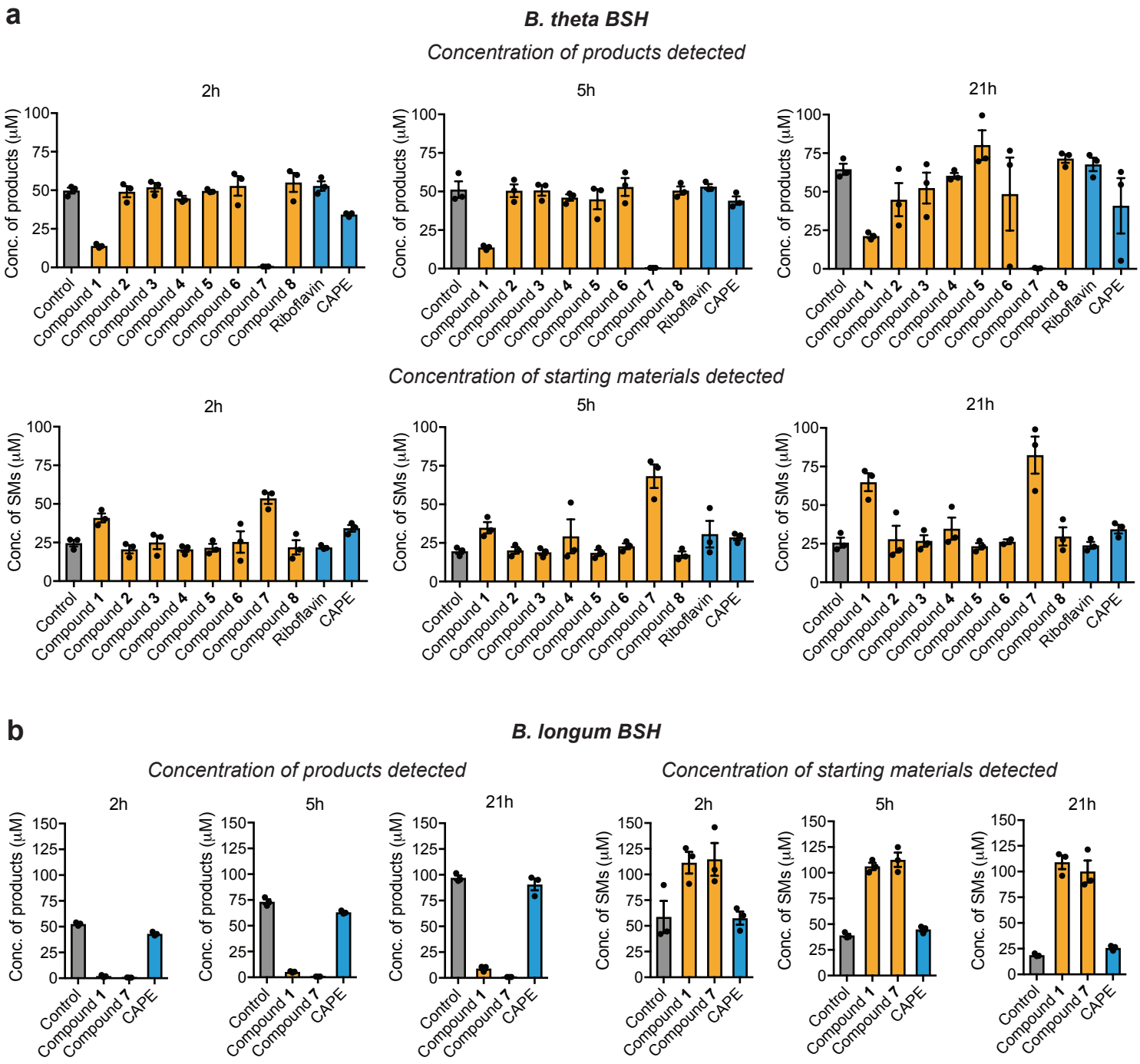

Supplementary Figure 4. Bile acid quantification for reporting % deconjugation, purified BSH proteins. Concentration of products formed (deconjugated bile acids) and unreacted starting materials (SMs) at each time point were determined for both *B. theta* BSH (**a**) and *B. longum* BSH (**b**) using UPLC-MS. % deconjugation for each sample was then determined using the following equation:
% deconjugation = Concentration of products / (Concentration of products + Concentration of starting materials)*100.
Note that no bile acids were detected in the reactions other than the starting materials (TCA, TβMCA, TUDCA and TDCA) and their deconjugated products (i.e., CA, βMCA, UDCA and DCA). Assays were performed in biological triplicate, and all data are presented as mean ± SEM.

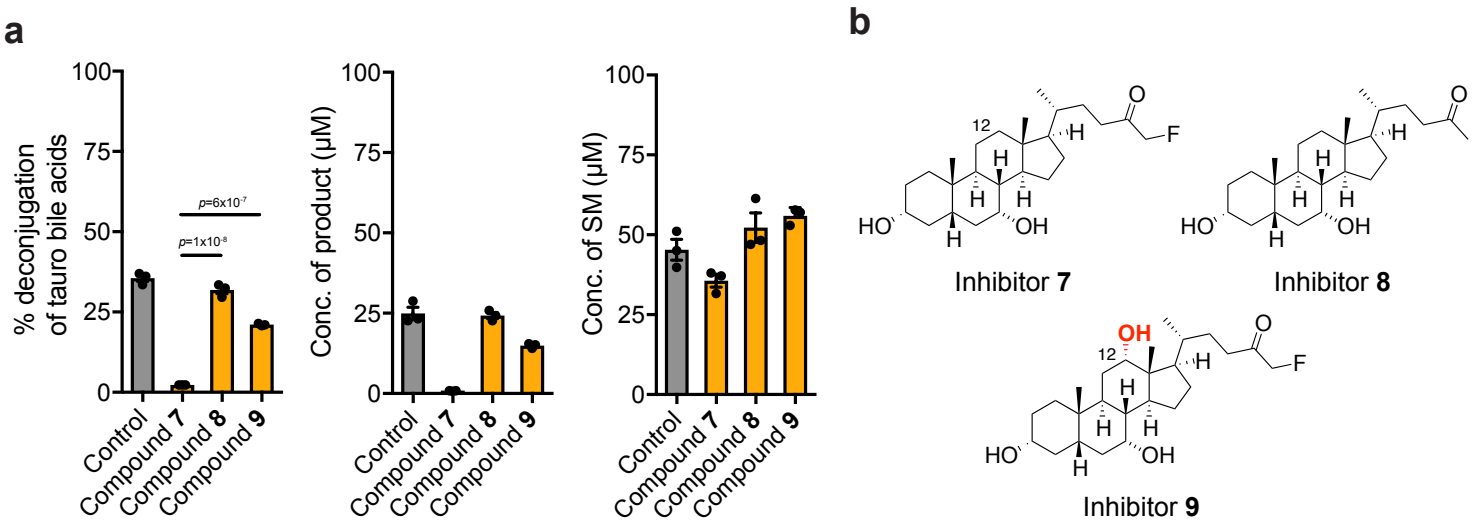

Supplementary Figure 5. Compound structure affects BSH inhibitory activity against growing *B. theta* cultures. (**a**) Compounds **8** and **9** are less potent inhibitors of *B. theta* BSH than compound **7**. Inhibitor (10 μM of compound **7**, **8**, or **9**) and 100 μM TUDCA were added to *B. theta* cultures at OD_{600} 0.1. Cultures were allowed to grow into stationary phase and percent deconjugation of tauro bile acids at 24h was determined by UPLC-MS. One-way ANOVA followed by Tukey's multiple comparisons test. Assays were performed in biological triplicate, and data are presented as mean ± SEM. (**b**) Structural comparison of compounds **7**, **8**, and **9**. Compound **8** lacks the α-FMK warhead, and compound **9** possesses a C12 = OH hydroxyl group.

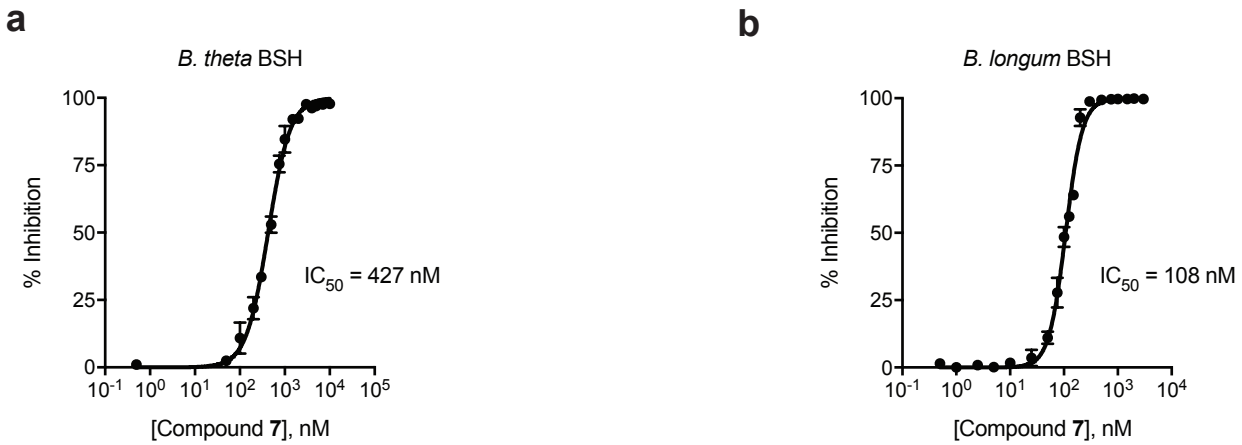

Supplementary Figure 6. Compound 7 is a potent inhibitor of recombinant BSHs. Dose-response curves and calculated IC_{50} values for compound **7**. 200 nM recombinant *B. theta* BSH (**a**, Gram negative) or *B. adolescentis* BSH (**b**, Gram positive) were pre-incubated with varying concentrations of compound **7** for 60 mins followed by the addition of conjugated bile acid substrate TUDCA and TDCA respectively. After a 2 h incubation, deconjugation was quantified using UPLC-MS. Assays were performed in biological triplicate, and all data are presented as mean ± SEM. Graphpad was used to fit IC_{50} curves.

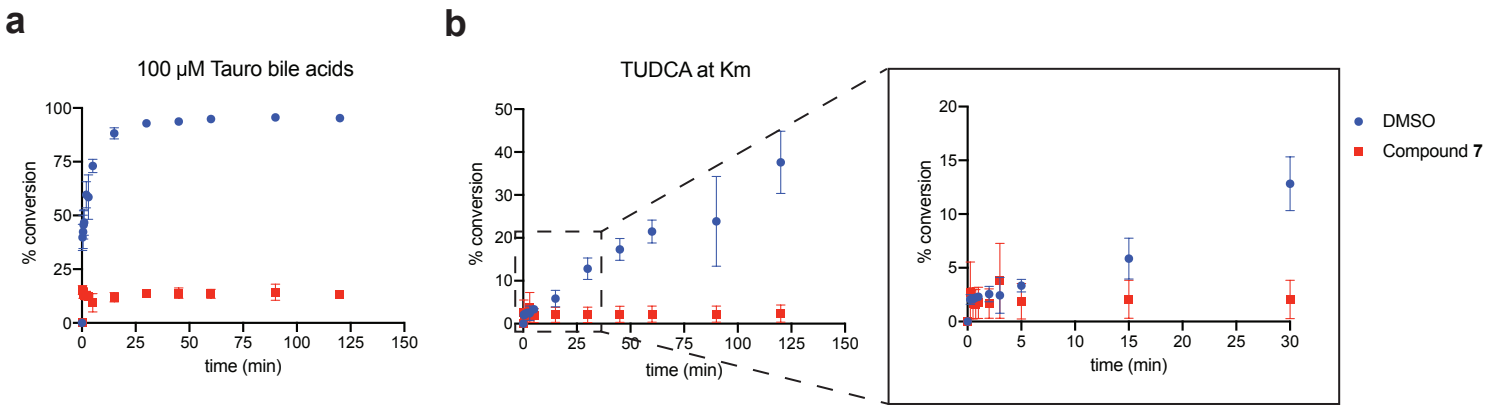

Supplementary Figure 7. Time required for complete inhibition of *B. theta* BSH.
(**a**) 100 µM compound **7** and conjugated bile acids (25 µM each of tauro-β-muricholic acid, TβMCA; tauro-cholic acid, TCA; tauro-ursodeoxycholic acid, TUDCA; and tauro-deoxycholic acid, TDCA) were added concomitantly to 200 nM rBSH with no preincubation period. Formation of deconjugated bile acid was measured using a UPLC-MS-based assay and reported as % conversion. In the presence of compound **7**, no increase in product formation was observed after 15 secs, indicating that enzyme activity was inhibited. (**b**) The assay in panel (**a**) was repeated using TUDCA, the substrate for which the *B. theta* BSH displayed the fastest turnover, at its K_m (8.2 mM) (see **Table 1**). In the presence of ~82 fold excess of substrate, no product formation was detected from 15 minutes onward in the compound **7**-treated condition, the earliest measurable timepoint for product formation.All assays were performed in biological triplicate, and data are presented as mean ± SEM.

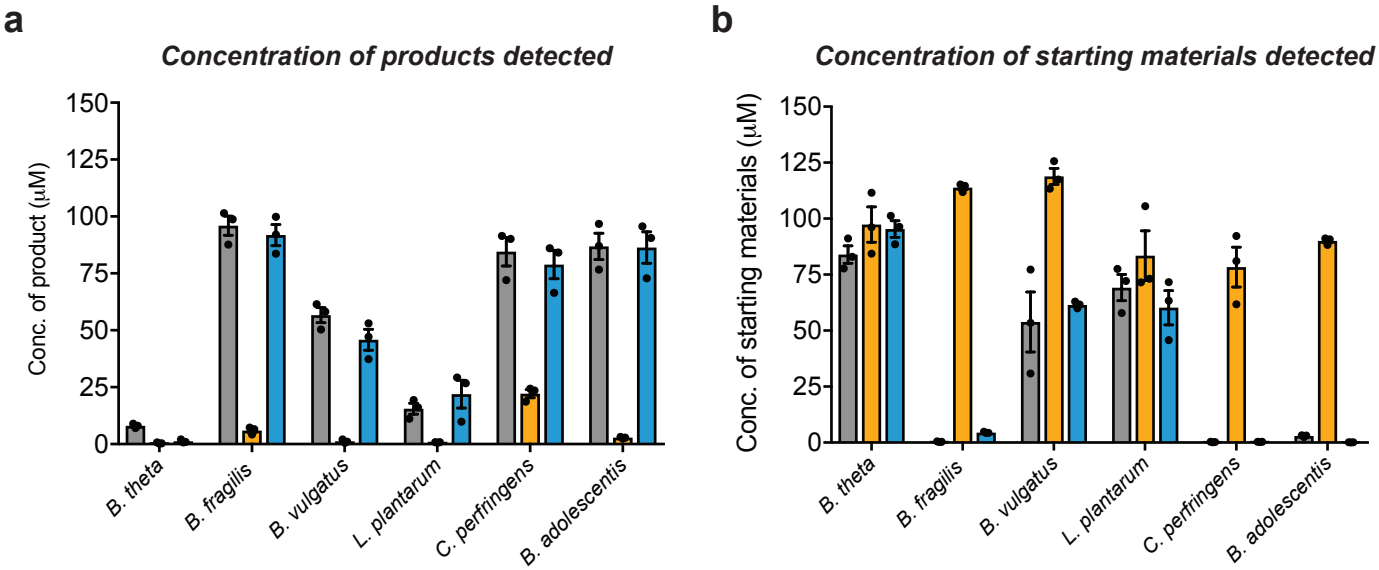

Supplementary Figure 8. Bile acid quantification for reporting % deconjugation, bacterial cultures. Concentration of products formed (deconjugated bile acids) (**a**) and unreacted starting materials (SMs) (**b**) in each culture were determined using UPLC-MS. % deconjugation for each sample was then determined using the following equation:

% deconjugation = Concentration of products / (Concentration of products + Concentration of starting materials)*100.

Note that for 5 of the 6 bacteria tested, no bile acids were detected in the cultures other than the starting materials (TCA, TβMCA, TUDCA and TDCA) and their deconjugated products (i.e., CA, βMCA, UDCA and DCA). For *B. fragilis*, these bile acids and one additional compound, 7-oxo-cholic acid (7-oxo-CA), were detected. 7-oxo-CA was quantified and included in the concentration of products in (**a**). Assays were performed in biological triplicate, and all data are presented as mean ± SEM.

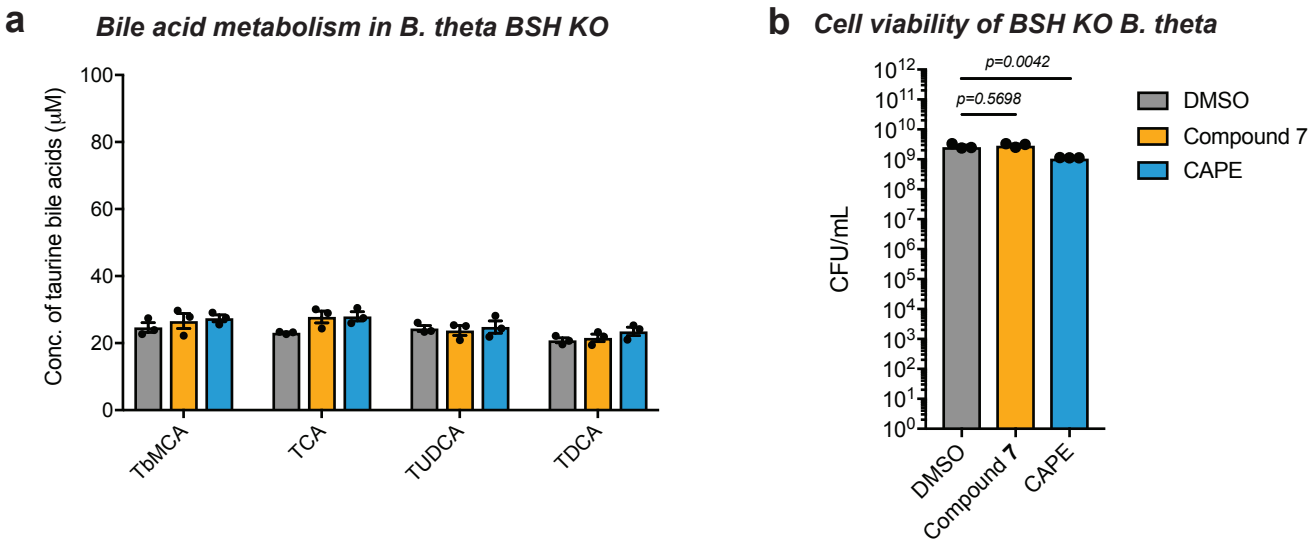

Supplementary Figure 9. **Compound 7 did not alter bile acid pools when incubated with *B.theta* BSH KO strain. (a**) 100 μM of a pool of taurine conjugated bile acids (TCA, TβMCA, TUDCA and TDCA, 25 μM each) and 100 μM inhibitor (compound 7 or CAPE) or DMSO were added to growing *B. theta*. Cultures were incubated for 24h and bile acid profiling was then performing using UPLC-MS. **No bile acids other than the starting materials** (TCA, TβMCA, TUDCA and TDCA) **were detected in any of the cultures.** (**b**) Colony forming units (CFUs) were determined from the assay in panel (**a**) after 24h. Compound **7** was not found to be bactericidal to BSH-deleted *B. theta* while CAPE was found to significantly affect the growth of this bacteria. For (**b**), one-way ANOVA followed by Dunnett's multiple comparison test. Assays were performed in biological triplicate, and data are represented as mean ± SEM.

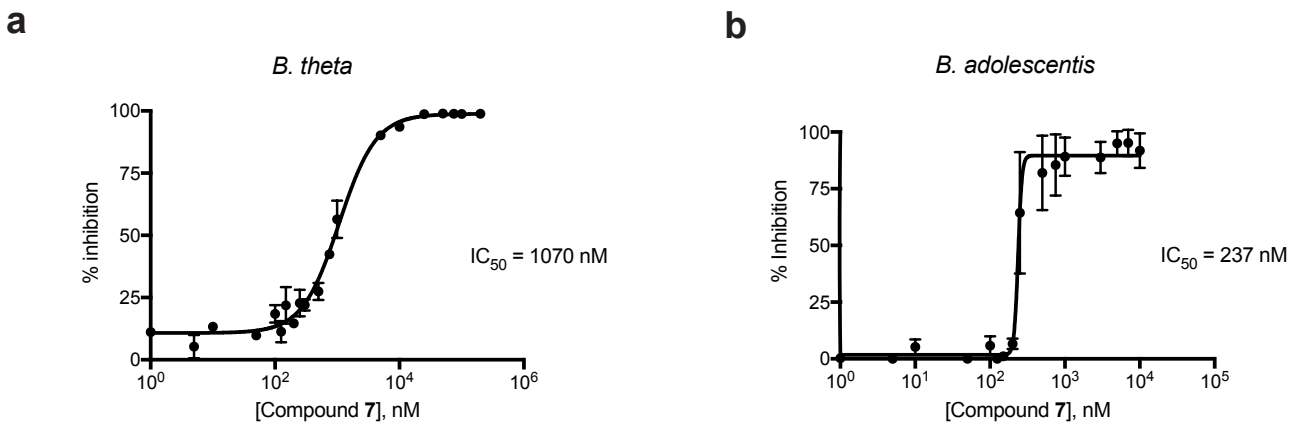

Supplementary Figure 10. Compound 7 is a potent BSH inhibitor in growing bacterial cultures. Dose-response curves and calculated IC_{50} values for compound **7**. Pre-log phase cultures of *B. theta* (**a**, Gram negative) and *B. adolescentis* (**b**, Gram positive) were incubated with conjugated substrate (TUDCA or TDCA) and allowed to grow anaerobically for 48h and 24h, respectively. Deconjugation was quantified using UPLC-MS. Assays were performed in biological triplicate, and all data are presented as mean ± SEM. Graphpad was used to fit IC_{50} curves.

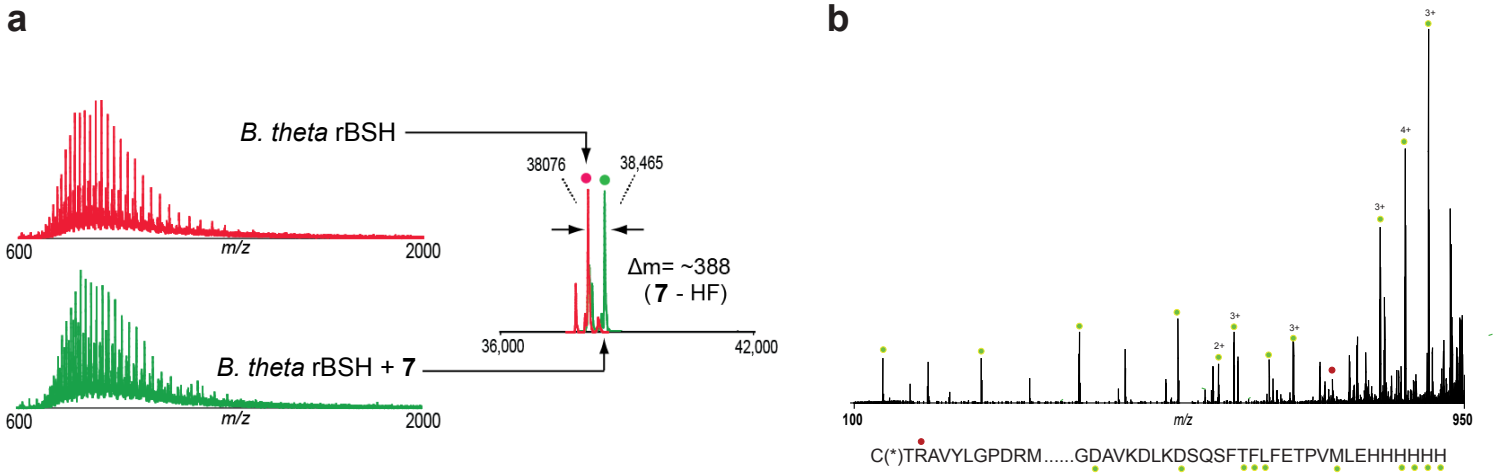

Supplementary Figure 11. Mass spectrometry revealed that compound 7 monolabels *B. theta* BSH. (**a**) Mass spectra (left) and zero-charge mass spectra (right) of BSH treated with DMSO (top, trace in red) or 10-fold excess of 7 for 2 h (bottom, trace in green). A shift in mass of 388 Da is consistent with covalent modification of BSH with a loss of HF. Two independent labeling reactions yielded similar results. (**b**) Top-down MS/MS of BSH treated with 10 fold excess of 7. Ions of type c and z are indicated with red and green glyphs respectively. Ion c3 indicates that modification is on the N-terminus Cys2 residue. Replicate analysis produced similar results.

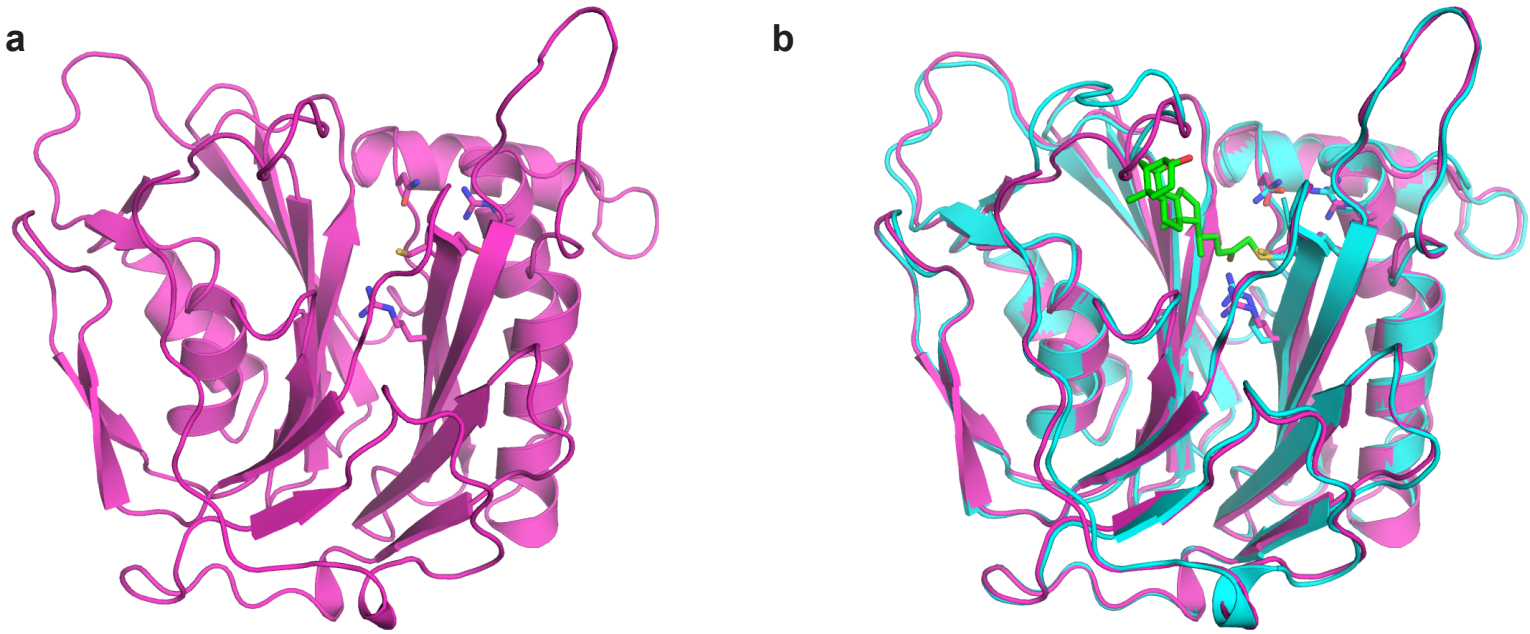

Supplementary Figure 12. Apo and co-crystal structures of B. theta BSH. X-ray structure of *B. theta* BSH apoprotein (**a**) superimposed on the X-ray structure of *B. theta* BSH covalently bound to compound **7** (**b**). The BSHs (apo in magenta, co-crystal structure in cyan) are shown in ribbon representation, with indicated side chains (magenta or cyan, respectively, with heteroatoms in CPK colors) rendered as sticks. Compound **7** (green, with heteroatoms in CPK colors) is rendered in stick form. Box (dashed lines) indicates loop (residues 127-138) that has repositioned in the co-crystal structure. Panels were prepared using PYMOL software (Schroedinger).

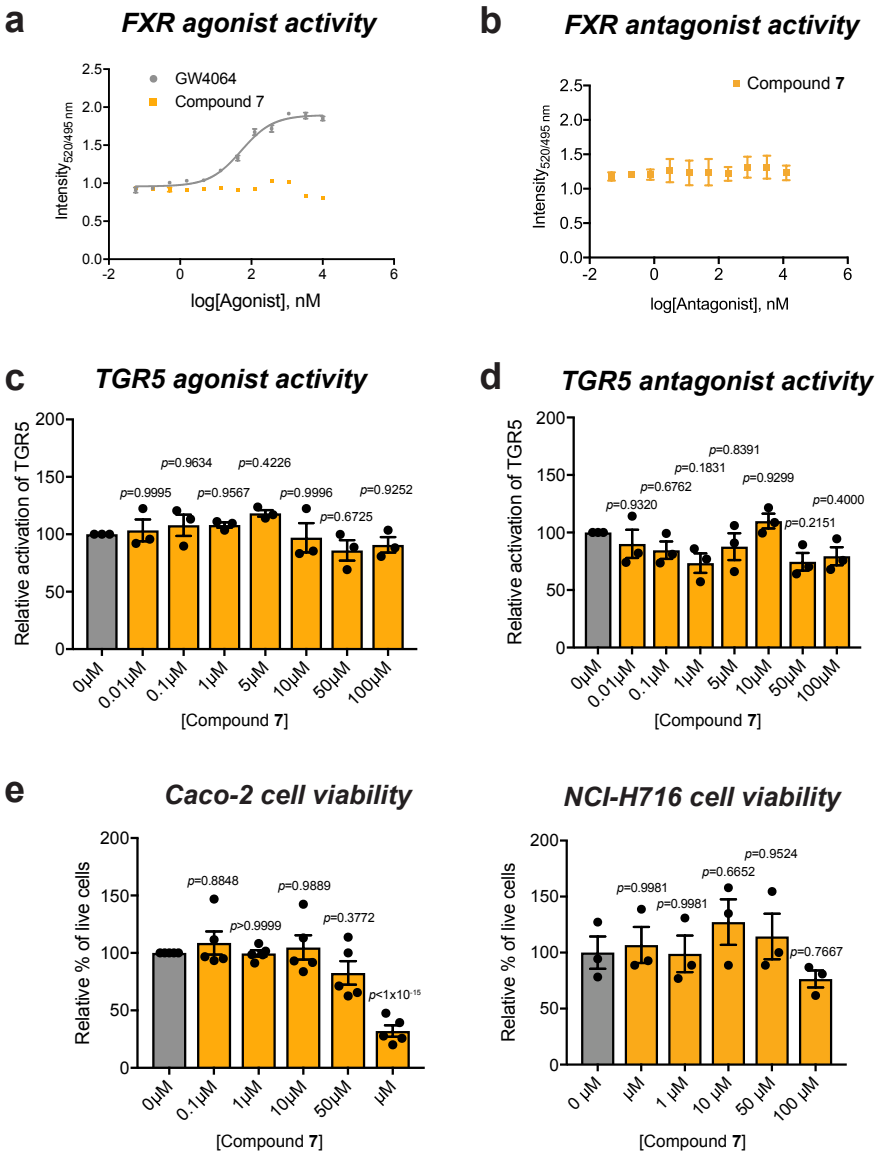

Supplementary Figure 13. Compound 7 is neither an agonist nor an antagonist of FXR or TGR5 and not toxic to human cells. (**a**) Compound **7** is not an farnesoid X receptor (FXR) agonist as determined by an FXR coactivator recruitment assay. n=4 biological replicates per concentration. (**b**) FXR antagonist activity of compound **7** was evaluated in the presence of FXR agonist GW4064 at its EC50 value (50 nM, as determined in the corresponding agonist assay). n=4 biological replicates per concentration. (**c**) Compound **7** is not a G protein-coupled bile acid receptor (GPBAR1 / TGR5) agonist. Endogenous TGR5 agonist activity was measured by incubating Caco-2 cells with varying concentrations of **7** overnight. n=3 biological replicates per concentration, one-way ANOVA followed by Dunnett's multiple comparisons test. (**d**) Endogenous TGR5 antagonist activity was measured by incubating Caco-2 cells with varying concentrations of compound **7** overnight in the presence of 10 μM of the TGR5 agonist LCA. n=3 biological replicates per concentration, one-way ANOVA followed by Dunnett's multiple comparisons test. (**e**) Compound **7** did not display toxicity toward Caco-2 or NCI-H716 cells at concentrations up to 50 μM and 100 μM, respectively. n=5 and n=3 biological replicates per concentration, respectively, one-way ANOVA followed by Dunnett's multiple comparisons test. All data are presented as mean ± SEM.

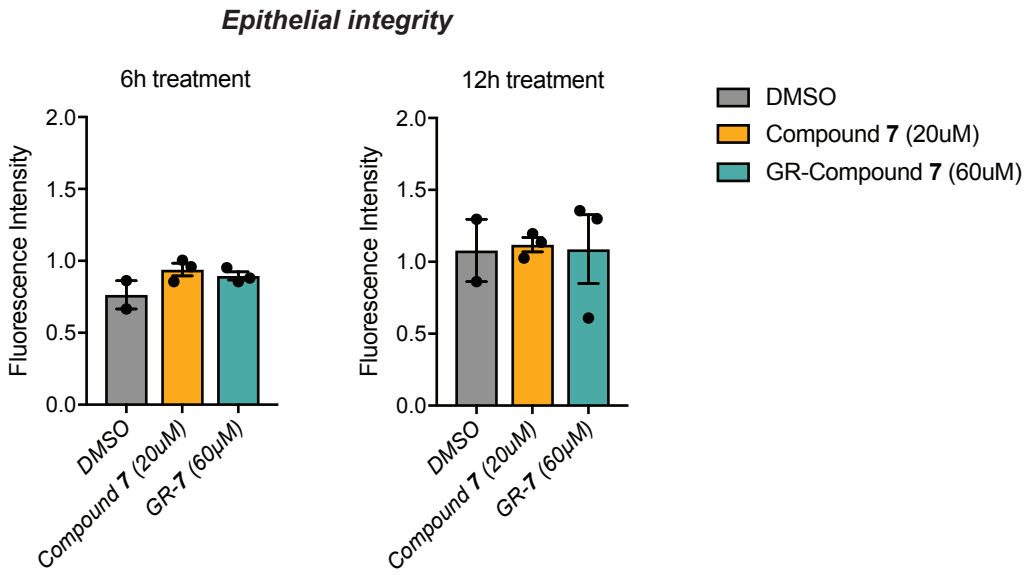

Supplementary Figure 14. Neither compound 7 nor GR-7 significantly affected epithelial barrier integrity. Incubation of compound **7** or GR-**7** with differentiated Caco-2 cells for 6 hours and 12 hours did not compromise epithelial monolayer integrity as measured by passive transport of 4 kDa FITC-dextran. n=2 biological replicates for DMSO control, n=3 biological replicates for inhibitor-treated conditions. All data are presented as mean ± SEM.

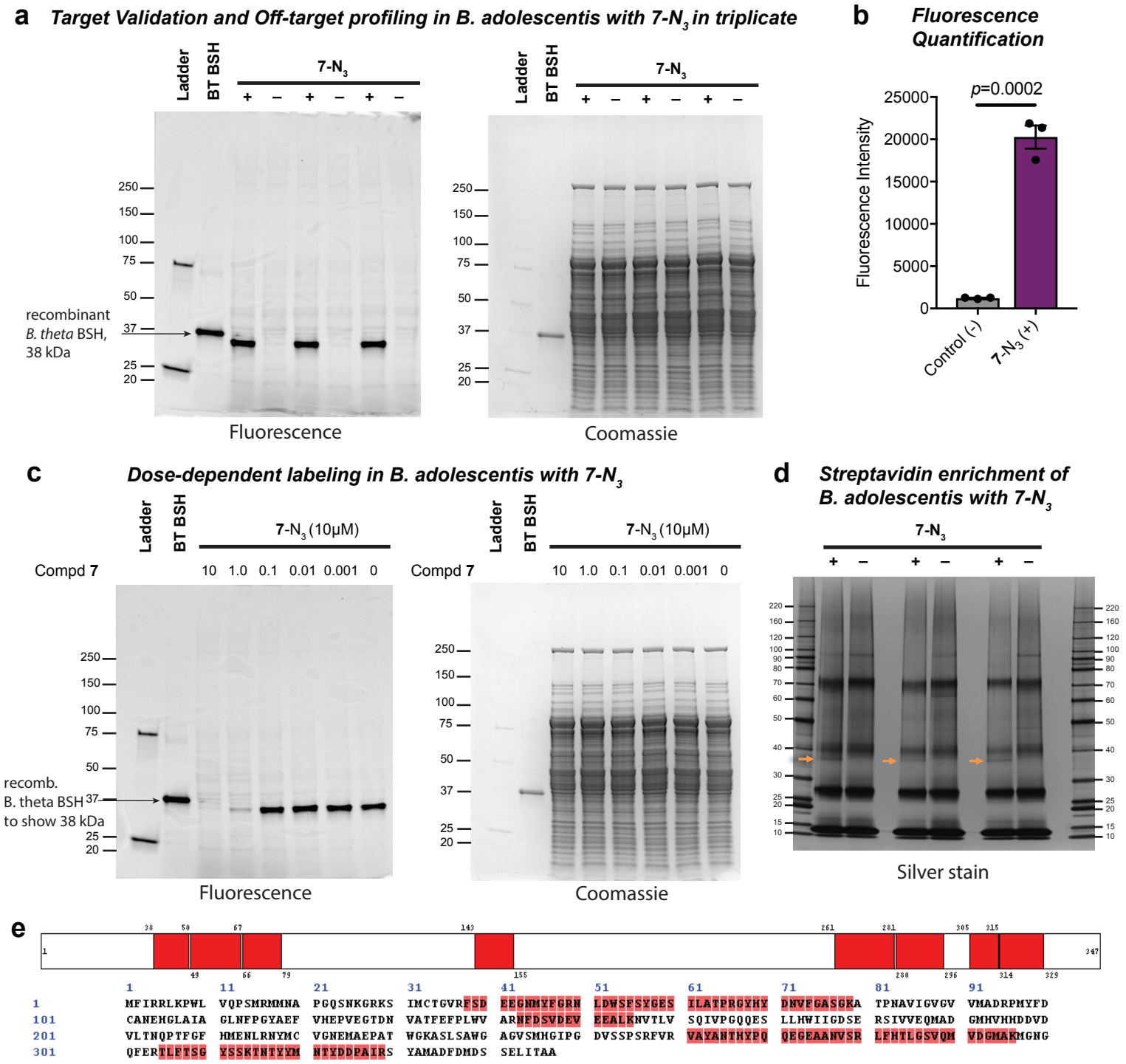

Supplementary Figure 15. Compound 7-N_3 labels *B. adolescentis* BSH with minimal off-target reactivity. (**a**) SDS-PAGE gel for the experiment described in **Fig. 4f** performed in biological triplicate (i.e., the treatment of *B. adolescentis* cultures with 10 μM compound **7**-N_3 for 1 hour and click reaction with Fluor 488-alkyne). Lysates were loaded at a concentration of 1.5 mg/mL. *B. theta* recombinant BSH (1 μM) was used as a positive control for the click reactions and as a standard to show 38 kDa. Ladder was diluted 100 fold and then loaded. (**b**) Fluorescence intensity of BSH bands were quantified. Two-tailed Student's t test. Data are presented as mean ± SEM. (**c**) Full SDS-PAGE gel for the experiment described in **Fig. 4h**. *B. adolescentis* cultures were treated with decreasing concentrations of compound **7** for 1 hour and then treated with 10 μM compound **7**-N_3 for an additional hour. Dose-dependent labeling of BSH was observed with decreasing concentrations of compound **7.** Experiment was repeated twice with similar results. (**d**) Silver stained gel for the experiment described in **Fig. 4g** performed in biological triplicate. (**e**) BSH derived tryptic peptides identified by LC-MS/MS analysis of in-gel digestion performed on bands indicated in (**d**). Amino acids highlighted in red map to tryptic peptides identified at a ~1% FDR.

Off-target profiling in mammalian cells with 7-N_3 in triplicate

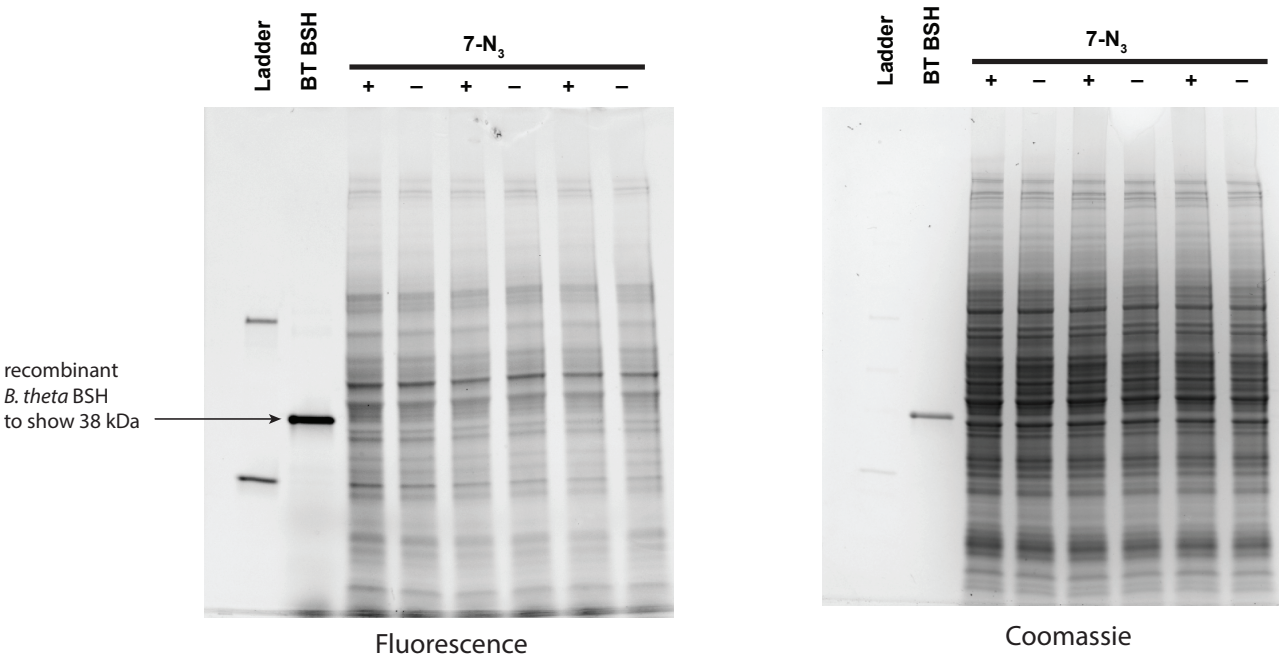

Supplementary Figure 16. 7-N_3 displayed minimal off-target labeling in mammalian cells. SDS-PAGE gel for the experiment described in **Fig. 4i** performed in biological triplicate (i.e., treatment of NCI-H716 cells with 10 μM **7**-N_3 for 1 hour followed by click reaction with Fluor 488-alkyne). Lysates were loaded at a concentration of 1.5 mg/mL. *B. theta* recombinant BSH (1 μM) was used as a positive control for the click reactions and as a standard to show 38 kDa. Ladder was diluted 100 fold and then loaded.

a

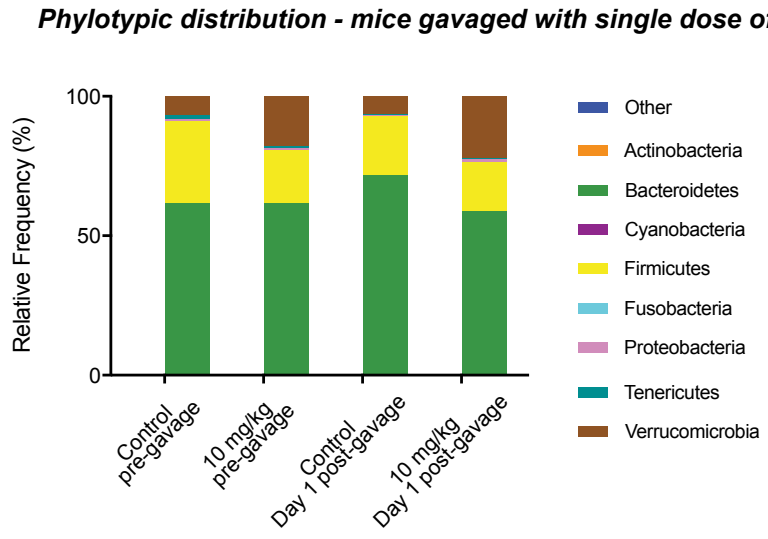

b

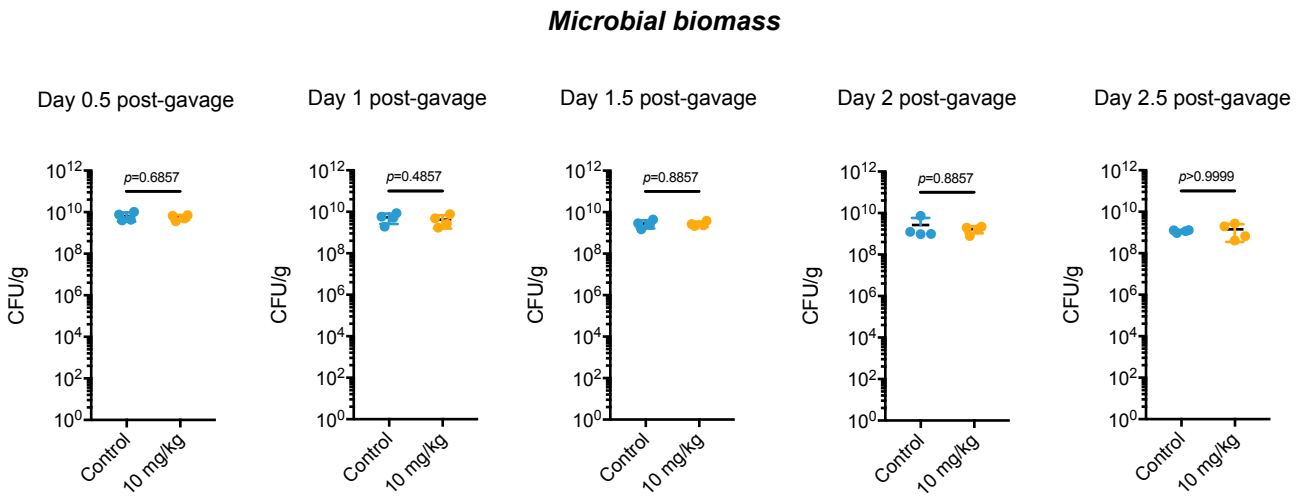

Supplementary Figure 17. Compound 7 did not significantly affect bacterial community composition or microbial biomass in vivo. (**a**) Average relative abundance of microbiota at the phylum level by taxon-based analyses, n=4 mice group. (**b**) CFU/g did not differ between the inhibitor- and vehicle-treated groups 0.5, 1,1.5, 2, or 2.5 days days post-gavage. n=4 mice per group, two-tailed Mann-Whitney test. All data are presented as mean ± SEM.

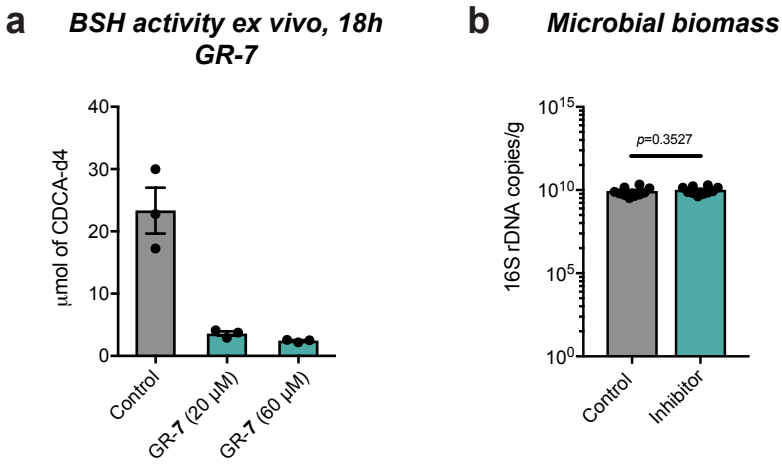

Supplementary Figure 18. Activity and in vivo effects of GR-7. (**a**) GR-**7** inhibited BSH activity in a fecal slurry. Freshly collected feces from conventional mice were resuspended in PBS (1 mg/mL) and incubated with 20 µM or 60 µM of GR-**7** for 30 mins. Glycochenodeoxycholic acid-d4 (GCDCA-*d*4, 100 µM) was added as substrate and formation of product was determined by UPLC-MS after 18 hours. Assays were performed in biological triplicate. (**b**) 16S rDNA copies/g in cecal contents 30 hours post-diet change. Microbial biomass did not differ between the inhibitor- and vehicle-treated groups. Two-tailed Mann-Whitney test. n=10 mice per group. All data are presented as mean ± SEM.

Synthetic Procedures

General: All anhydrous reactions were run under a positive pressure of argon or nitrogen. Anhydrous methylene chloride (DCM) and tetrahydrofuran (THF) were purchased from Sigma Aldrich. Silica gel column chromatography was performed using 60 Å silica gel (230−400 mesh). NMR spectra recorded in $CDCl_3$ used residual chloroform or TMS as the internal reference.

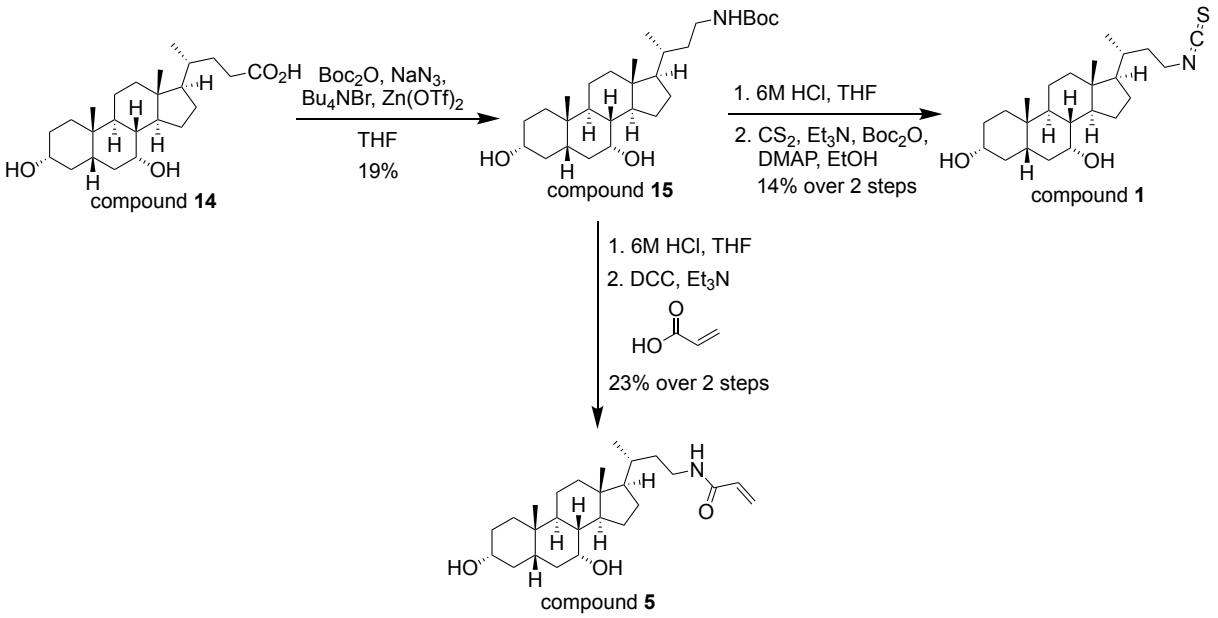

Scheme 1. Synthesis of compounds 1 and 5.

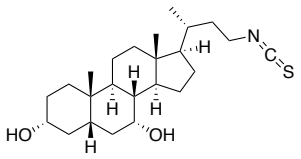

Compound **1.**

Step 1. To a solution of chenodeoxycholic acid (0.5 g, 1.27 mmol), sodium azide (0.29 g, 4.44 mmol), tetrabutylammonium bromide (61.0 mg, 0.19 mmol) and zinc trifluoromethanesulfonate (18.0 mg, 0.05 mmol) in 4.3 mL anhydrous THF at 40 °C was added di-tert-butyl dicarbonate

(0.3 g, 1.40 mmol) and the mixture was heated overnight. The mixture was cooled to room temperature (rt) and quenched with 10 mL of 10% sodium nitrite and then diluted with 10 mL ethyl acetate. The organic layer was separated and the aqueous layer was extracted with ethyl acetate (2 x 10 mL). The combined organic layers where then dried over magnesium sulfate, filtered and concentrated on the rotovap. The crude compound was then purified by silica gel chromatography (80% ethyl acetate/20% hexanes) to provide compound **15** (0.11 g, 19%) as a white foam.

Step 2. To the Boc amine **15** (0.97 g, 2.09 mmol) in 4 mL THF, 1 mL of 6M HCl was added and the mixture was refluxed for 45 mins. The mixture was then cooled to rt and concentrated on the rotovap. The aqueous solution was then resuspended in 10 mL ethyl acetate and basified to pH 10 with 1M sodium hydroxide. The organic layer was separated and the aqueous layer was extracted with ethyl acetate (2 x 10 mL). The combined organic layers where then dried over sodium sulfate, filtered and concentrated to provide the free amine (0.51 g, 67%) which was used in the subsequent steps without further purification.

Step 3. A literature reported protocol was followed for the final step of the synthesis – *Tetrahedron Lett.,* **2008**, *49*, 3117-3119.

Briefly, to the amine (0.24 g, 0.66 mmol) in 2 mL ethanol, carbon disulphide (0.40 ml, 6.6 mmol) and trimethylamine (0.1 mL, 0.66 mmol) were added and the mixture was stirred at rt for 1h. The solution was then cooled to 0 °C and di-tert-butyl dicarbonate (0.14 g, 0.66 mmol) and DMAP (4.0 mg, 0.03 mmol) were added and the resulting mixture was stirred at 0 °C for 10 mins. The mixture was then warmed to rt and stirred for 10 mins following which it was concentrated on the rotovap. The crude compound was then purified by silica gel

chromatography (75% ethyl acetate/25% hexanes) to provide the compound **1** (20.0 mg, 20%) as a clear oil.

Compound 1. TLC (Ethyl acetate:Hexanes, 85:15 v/v): $R_f = 0.5$; ^{1}H NMR (400 MHz, $CDCl_3$): δ 3.83 (s, 1H), 3.57-3.41 (m, 3H), 2.18 (q, *J* = 12.4 Hz, 1H), 1.99-1.79 (m, 7H), 1.71-1.64 (m, 3H), 1.57-1.11 (m, 14H), 1.00-0.81 (m, 7H), 0.67 (s, 3H); ^{13}C NMR (100 MHz, $CDCl_3$): δ 71.97, 68.50, 68.42, 55.85, 50.44, 42.80, 42.75, 41.44, 39.88, 39.60, 39.38, 36.13, 35.30, 35.03, 34.69, 33.49, 32.82, 30.66, 28.25, 23.67, 22.75, 20.56, 18.20, 11.73; HRMS (*m/z*): $[M - 2H_2O + H]^+$ calcd. for $C_{24}H_{39}NO_2S$, 370.2568; found, 370.2543.

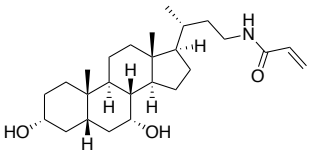

Compound **5.**

Step 1. The free amine was synthesized as per the conditions in step 2 for compound **1**.

Step 2. The acid (12.0 mg, 0.16 mmol) was dissolved in 1.65 mL anhydrous DCM followed by the addition of the coupling agent N,N'-dicyclohexylcarbodiimide (DCC) (42.0 mg, 0.20 mmol) and trimethylamine (76 µL, 0.55 mmol). The mixture was stirred at rt for 30 mins and then the free amine (50.0 mg, 0.14 mmol) dissolved in 1.4 mL DCM was added to the above mixture. The resulting solution was stirred at rt for 3 h. The mixture was then partitioned using 5 mL of 1M HCl and 5 mL DCM. The organic layer was separated and the aqueous layer was extracted with DCM (2 x 10 mL). The combined organic layers where then dried over sodium sulfate, filtered and concentrated. The crude compound was then purified by silica gel chromatography (90% ethyl acetate/10% hexanes) to provide the compound **5** (20.0 mg, 33%) as a clear oil.

Compound 5. TLC (Ethyl acetate:Hexanes, 80:20 v/v): R_f = 0.12; ^{1}H NMR (400 MHz, $CDCl_3$): δ 6.27 (dd, *J* = 16.8, 1.2 Hz, 1H), 6.07 (dd, *J* = 16.8, 10.4 Hz, 1H), 5.62 (dd, *J* = 10.4, 1.2 Hz, 1H), 5.45 (br s, 1H), 3.85-3.84 (m, 1H), 3.50-3.37 (m, 2H), 3.31-3.22 (m, 1H), 2.20 (q, *J* = 12.8 Hz, 1H), 2.01-1.79 (m, 5H), 1.73-1.10 (m, 19H), 1.01-0.94 (m, 4H), 0.90 (s, 3H), 0.66 (s, 3H); ^{13}C NMR (100 MHz, $CDCl_3$): δ 155.54, 130.95, 126.14, 72.00, 68.51, 55.97, 50.45, 42.73, 41.46, 39.91, 39.61, 39.42, 37.24, 35.76, 35.30, 35.03, 34.61, 34.07, 32.83, 30.68, 28.35, 23.69, 22.75, 20.55, 18.67, 11.73; HRMS (*m/z*): $[M - 2H_2O + H]^+$ calcd. for $C_{26}H_{43}NO_3$, 382.3110; found, 382.3082.

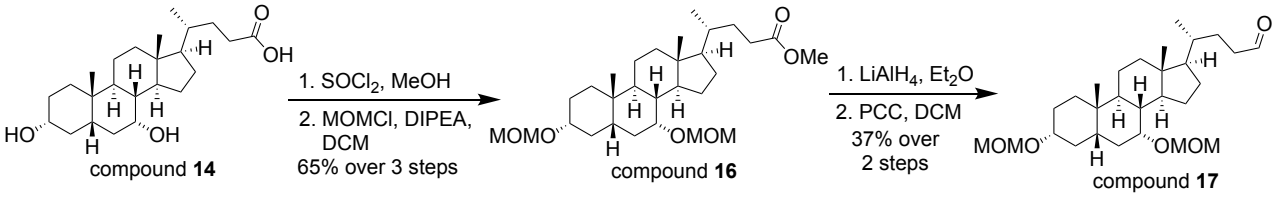

Scheme 2. Synthesis of the common C-24 aldehyde intermediate 17.

Step 1. To chenodeoxycholic acid (20.0 g, 50.8 mmol) suspended in 100 mL methanol at 0 °C, thionyl chloride (4.0 mL, 55.9 mmol) was added dropwise. The reaction was warmed to rt and stirred for 3 h. The reaction was quenched by the addition of 100 mL saturated sodium bicarbonate. The resulting mixture was then concentrated on the rotovap. The residue was partitioned between aqueous layer and 50 mL ethyl acetate. The organic layer was separated and the aqueous layer was extracted with ethyl acetate (2 x 50 mL). The combined organic layers where then dried over sodium sulfate, filtered and concentrated on the rotovap. The crude compound was then purified by silica gel chromatography (60% ethyl acetate/ 40% hexanes) to provide the methyl ester (20.6 g, quant.) as a white foam.

Step 2. The methyl ester (1.6 g, 3.93 mmol) was dissolved in 8 mL of anhydrous DCM and cooled to 0 °C under nitrogen. To this solution, *N,N*-diisopropylethylamine (1.4 mL, 11.79 mmol) was added followed by the slow addition of methoxymethyl chloride (1.2 mL, 11.79 mmol). The reaction mixture was then warmed to rt and stirred for 3 h. The reaction was quenched with the addition of 10 mL saturated sodium bicarbonate. The organic layer was separated and the aqueous layer was extracted with DCM (2 x 10 mL). The combined organic layers were then dried over sodium sulfate, filtered and concentrated. The crude compound was then purified by silica gel chromatography (25% ethyl acetate/75% hexanes) to provide the pure product **16** (1.26 g, 65%) as a white foam.

Step 3. The protected methyl ester **16** (1.73 g, 3.49 mmol) was dissolved in 14 mL anhydrous diethyl ether and cooled to 0 °C under nitrogen. LiAlH4 (0.27, 6.99 mmol) was added in portions to the above solution. The mixture was allowed to stir at 0 °C for 2 h and then quenched by the slow addition of 14mL of Rochelle's salt. The organic layer was separated and the aqueous layer was extracted with ethyl acetate (2 x 15 mL). The combined organic layers were then dried over magnesium sulfate, filtered and concentrated. The crude compound was then purified by silica gel chromatography (30% ethyl acetate/70% hexanes) to provide the pure C-24 alcohol (0.80 g, 50%) as a clear oil.

Step 4. To a suspension of pyridinium chlorochromate (1.42 g, 6.57 mmol) and silica gel (1.42 g) in 8 mL DCM at 0 °C, C-24 alcohol (1.9 g, 4.06 mmol) dissolved in another 8 mL DCM was added slowly. The resulting solution was then stirred at rt for 2 h. The reaction mixture was then filtered through a bed of celite and the residue was concentrated to provide the crude aldehyde **S4**. The crude compound was then purified by silica gel chromatography (20% ethyl acetate/80% hexanes) to provide pure aldehyde **17** (1.39 g, 74%) as a clear oil.

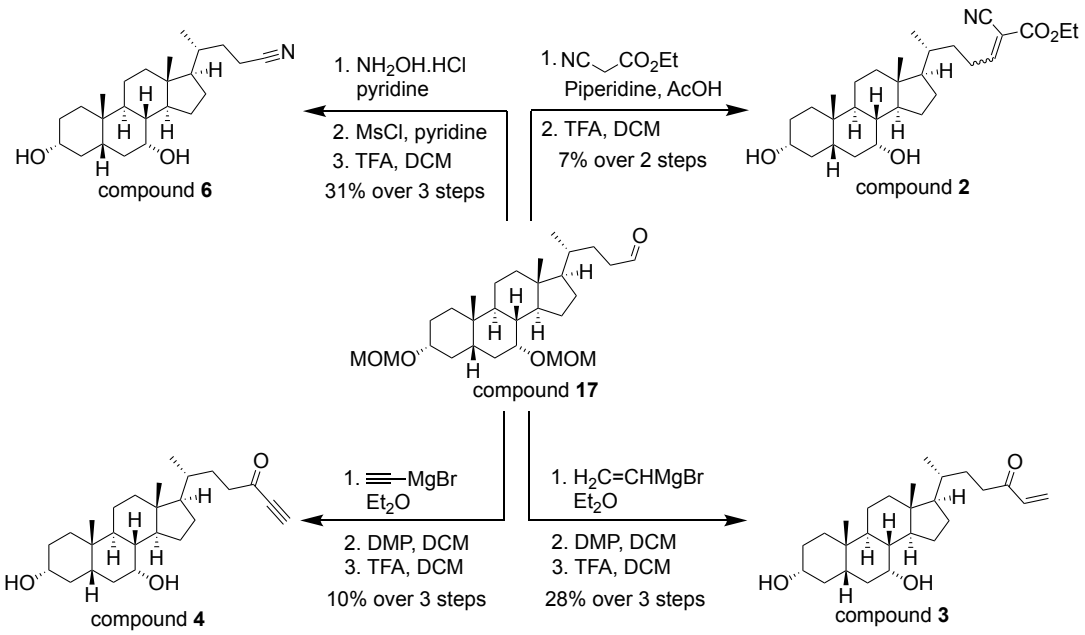

Scheme 3. Synthesis of compounds 2-4 and 6.

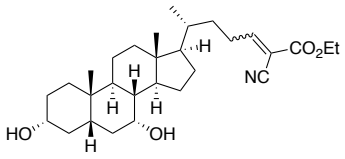

Compound **2.**

Step 1. A literature reported protocol was followed for this step of the synthesis – *J. Med. Chem.*, **2005**, *48*, 3026-3035.

To the aldehyde **17** (0.12 g, 0.28 mmol) and ethyl 2-cyanoacrylate (35.0 mg, 0.30 mmol) at 0 °C, acetic acid (17 µL, 0.28 mmol) and piperidine (28 µL, 0.28 mmol) were added. The mixture was then stirred at rt overnight. The residue was then diluted with 5 mL DCM and washed with 5 mL of 1M HCl. The organic layer was separated and the aqueous layer was extracted with DCM (2 x 10 mL). The combined organic layers were then dried over sodium sulfate, filtered and concentrated. The crude compound was then purified by silica gel chromatography (30% ethyl acetate/70% hexanes) to provide the condensed intermediate (40.0 mg, 29%) as a clear oil.

Step 2. To the condensed product (50.0 mg, 0.09 mmol) in 1 mL DCM, 0.2 mL trifluoroacetic acid was added and the reaction mixture was stirred at 0 °C for 1 h. The mixture was then cooled to rt, diluted with 5 mL DCM and quenched slowly with 5 mL saturated sodium bicarbonate solution. The organic layer was separated and the aqueous layer was extracted with DCM (2 x 10 mL). The combined organic layers were then dried over sodium sulfate, filtered and concentrated. The crude compound was then purified by silica gel chromatography (60% ethyl acetate/40% hexanes) to provide the target compound **2** (10.0 mg, 24%) as a mixture of diastereomers which was used in the screen without further purification.

Compound 2. TLC (Ethyl acetate:Hexanes, 70:30 v/v): $R_f = 0.43$; ^{1}H NMR (400 MHz, $CDCl_3$): δ 7.64 (t, J = 8.0 Hz, 1H), 4.31 (q, J = 7.2 Hz, 2H), 3.85 (s, 1H), 3.50-3.44 (m, 1H), 2.63-2.43 (m, 2H), 2.20 (q, J = 12.8 Hz, 1H), 1.99-1.11 (m, 26H), 1.02-0.98 (m, 4H), 0.91 (s, 4H), 0.66 (s, 3H); ^{13}C NMR (100 MHz, $CDCl_3$): Because this compound was isolated as a mixture of diastereomers, C13 peak assignment was not performed. HRMS (*m/z*): $[M + Na]^+$ calcd. for $C_{29}H_{45}NO_4$, 494.3246; found, 494.3233.

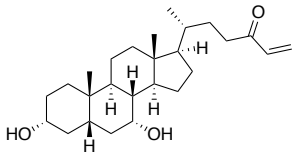

Compound **3.**

Step 1. In a flame dried flask, the aldehyde **17** (0.50 g, 1.07 mmol) was dissolved in 4.3 mL diethyl ether under nitrogen. Vinylmagnesium bromide (1.6 mL, 1.60 mmol) was then added slowly to the above solution at 0 °C. The mixture was stirred at rt overnight. The reaction was quenched by the addition of 5 mL 1M HCl and diluted with 10 mL ethyl acetate. The organic layer was separated and the aqueous layer was extracted with ethyl acetate (2 x 10 mL). The

combined organic layers were then dried over magnesium sulfate, filtered and concentrated. The crude compound was then purified by silica gel chromatography (30% ethyl acetate/70% hexanes) to provide the alcohol as a mixture of diastereomers (0.40 g, 77%).

Step 2 and 3. Compound **3,** was synthesized following Steps 2 and 3 as described above for compound **4**. The overall yield is reported on the reaction scheme.

Compound 3. TLC (Ethyl acetate:Hexanes, 60:40 v/v): $R_f = 0.34$; ^{1}H NMR (400 MHz, $CDCl_3$): δ 6.35 (dd, *J* = 18.0, 10.8 Hz, 1H), 6.21 (dd, *J* = 17.6, 1.2 Hz, 1H), 5.89 (dd, *J* = 10.4, 0.8 Hz, 1H), 3.86-3.85 (m, 1H), 3.50-3.43 (m, 1H), 2.65-2.57 (m, 1H), 2.54-2.46 (m, 1H), 2.20 (q, *J* = 12.8 Hz, 1H), 2.01-1.11 (m, 22H), 1.02-0.91 (m, 9H), 0.66 (s, 3H); ^{13}C NMR (100 MHz, $CDCl_3$): δ 201.43, 136.57, 127.77, 72.01, 68.53, 55.78, 50.46, 42.70, 41.47, 39.91, 39.62, 39.42, 36.51, 35.35, 35.31, 35.04, 34.60, 32.84, 30.67, 30.02, 28.15, 23.71, 22.75, 20.57, 18.47, 11.77; HRMS (*m/z*): $[M - 2H_2O + H]^+$ calcd. for $C_{26}H_{42}O_3$, 367.3001; found, 367.2985.

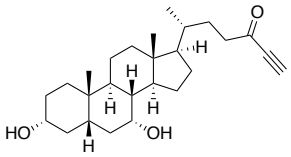

Compound **4**.

Step 1. In a flame dried flask, the aldehyde **17** (0.20 g, 0.65 mmol) was dissolved in 1.5 mL diethyl ether under nitrogen. Ethynylmagnesium bromide (1.2 mL, 0.97 mmol) was then added slowly to the above solution at 0 °C. The mixture was stirred at rt overnight. The reaction was quenched by the addition of 2 mL 1M HCl and diluted with 10 mL ethyl acetate. The organic layer was separated and the aqueous layer was extracted with ethyl acetate (2 x 10 mL). The combined organic layers were then dried over magnesium sulfate, filtered and concentrated.

The crude compound was then purified by silica gel chromatography (30% ethyl acetate/70% hexanes) to provide the alcohol as a mixture of diastereomers (0.12 g, 57%).

Step 2. To the alcohol (0.12 g, 0.24 mmol) in 2.5 mL anhydrous DCM at 0 °C, Dess-Martin periodinane (1.1 mL, 0.37 mmol) was added slowly. The reaction mixture was then stirred at rt until the reaction was complete by TLC. Upon consumption of the starting material, the reaction was quenched by the addition of 3 mL saturated sodium thiosulfate solution and 3 mL saturated sodium bicarbonate solution. The organic layer was separated and the aqueous layer was extracted with DCM (2 x 10 mL). The combined organic layers were then dried over sodium sulfate, filtered and concentrated. The crude compound was then purified by to provide the product (60.0 mg, 50%) as a clear oil.

Step 3. To the protected compound (20.0 mg, 0.04 mmol) in 1.0 mL DCM, trifluoroacetic acid (12 μL, 0.15 mmol) was added and the reaction mixture was stirred at 0 °C for 1 h. The mixture was then cooled to rt, diluted with 5 mL DCM and quenched slowly with 5 mL saturated sodium bicarbonate solution. The organic layer was separated and the aqueous layer was extracted with DCM (2 x 10 mL). The combined organic layers were then dried over sodium sulfate, filtered and concentrated. The crude compound was then purified by silica gel chromatography (50% ethyl acetate/50% hexanes) to provide the target compound **4** (5.5 mg, 34%) as a clear oil.

Compound 4. TLC (Ethyl acetate:Hexanes, 60:40 v/v): $R_f = 0.28$; ^{1}H NMR (400 MHz, $CDCl_3$): δ 3.86-3.85 (m, 1H), 3.50-3.43 (m, 1H), 3.20 (s, 1H), 2.66-2.48 (m, 2H), 2.20 (q, J = 12.8 Hz, 1H), 2.02-1.80 (m, 6H), 1.73-1.11 (m, 18H), 1.02-0.91 (m, 7H), 0.66 (s, 3H); ^{13}C NMR (100 MHz, $CDCl_3$): δ 187.87, 78.23, 72.00, 68.52, 55.71, 50.46, 42.72, 42.44, 41.46, 39.91, 39.60, 39.42, 35.30, 35.14, 35.03, 35.02, 34.63, 32.83, 30.67, 29.73, 28.11, 23.69, 22.75, 20.56, 18.33, 11.76; HRMS (*m/z*): $[M - 2H_2O + H]^+$ calcd. for $C_{26}H_{40}O_3$, 365.2844; found, 365.2827.

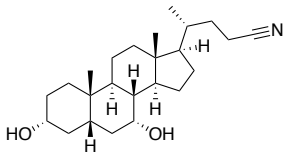

Compound **6**.

Step 1. To the aldehyde **17** (0.50 g, 1.07 mmol) in 4 mL anhydrous pyridine, hydroxylamine hydrochloride (0.37 g, 5.37 mmol) was added and the reaction mixture was stirred at rt for 4 h. The mixture was then diluted with 20 mL DCM and washed with 20 mL 1M HCl. The organic layer was separated and the aqueous layer was extracted with DCM (2 x 20 mL). The combined organic layers were then dried over sodium sulfate, filtered and concentrated to provide the crude oxime which was used in the subsequent step without further purification.

Step 2. To the oxime (0.38 g, 0.79 mmol) in 4 mL pyridine, methanesulfonyl chloride (92 μL, 1.19 mmol) was added at 0 °C. The reaction mixture was warmed to rt and stirred for 18 h after which the mixture was diluted with 20 mL DCM and washed with 20 mL 1M HCl. The organic layer was separated and the aqueous layer was extracted with DCM (2 x 20 mL). The combined organic layers were then dried over sodium sulfate, filtered and concentrated to provide the crude oxime which was purified using silica gel chromatography (20% ethyl acetate/80% hexanes) to provide the pure bis-MOM protected nitrile (0.16g, 44% yield over two steps).

Step 3. To the protected nitrile (70.0 mg, 0.15 mmol) in 1.5 mL tetrahydrofuran (THF), 50% HBr (100 μL, 0.61 mmol) was added and the reaction mixture was heated at 50 °C for 1 h. The mixture was then cooled to rt and diluted with 5 mL ethyl acetate and then quenched slowly with 5 mL saturated sodium bicarbonate solution. The organic layer was separated and the aqueous layer was extracted with ethyl acetate (2 x 20 mL). The combined organic layers were then dried over magnesium sulfate, filtered and concentrated. The crude compound was then

purified by silica gel chromatography to provide the target compound **6** (40.0 mg, 71%) as a white solid.

Compound 6. TLC (Ethyl acetate:Hexanes, 60:40 v/v): $R_f = 0.2$; ^{1}H NMR (400 MHz, $CDCl_3$): δ 3.843-3.836 (m, 1H), 3.49-3.41 (m, 1H), 2.40-2.15 (m, 3H), 2.00-1.80 (m, 6H), 1.72-1.63 (m, 3H), 1.55-1.11 (m, 15H), 1.01-0.90 (m, 7H), 0.67 (s, 3H); ^{13}C NMR (100 MHz, $CDCl_3$): δ 120.17, 71.94, 68.42, 55.54, 50.42, 42.77, 41.44, 39.86, 39.59, 39.36, 35.30, 35.17, 35.02, 34.71, 32.81, 31.51, 30.65, 28.15, 23.65, 22.74, 20.55, 17.86, 14.25, 11.77; HRMS (*m/z*): $[M - 2H_2O + H]^+$ calcd. for $C_{24}H_{39}NO_2$, 338.2848; found, 338.2828.

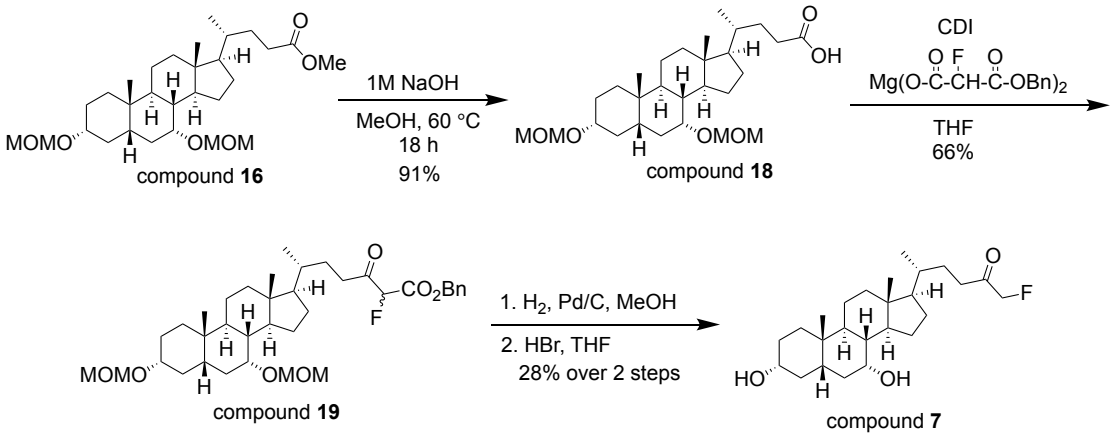

Scheme 4. Synthesis of compound 7.

The magnesium benzyl fluoromalonate coupling reagent was synthesized according to a reported protocol: James T Palmer. Process for Forming a Fluoromethyl Ketone. 5,210,272, May 11, 1993.

Step 1. To the protected methyl ester **16** (6.4 g, 12.95 mmol) in 26 mL methanol, 28 mL 1M NaOH was added and the resulting solution was heated to 60 °C overnight. The mixture was then concentrated on the rotovap and resuspended in 30 mL each of 1M HCl and DCM. The organic layer was separated and the aqueous layer was extracted with DCM (2 x 30 mL). The

combined organic layers were then dried over sodium sulfate, filtered and concentrated to provide the acid **18** (5.7 g, 91%) as a white foam, which was used in subsequent reactions without further purification.

Step 2. To the C-24 acid **18** (1.60 g, 3.33 mmol) in 6.5 mL of anhydrous THF, 1'-carbonyldiimidazole (CDI) (0.7 g, 4.33 mmol) was added and stirred at rt for 1 h. The magnesium benzyl fluoromalonate (1.20 g, 2.68 mmol) was suspended in 6.5 mL anhydrous THF and the above solution was added dropwise and the resulting mixture was stirred at rt for 18 h. The reaction was quenched by the addition of 10 mL of 1M HCl and concentrated on the rotovap. The residue was then partitioned using 10 mL DCM and 10 mL water. The organic layer was separated and the aqueous layer was extracted with DCM (2 x 10 mL). The combined organic layers were then dried over sodium sulfate, filtered and concentrated. The crude compound was then purified by silica gel chromatography (20% ethyl acetate/80% hexanes) to provide the pure compound **19** (1.36 g, 66%) as a white foam.

Step 3. The compound **19** (1.0 g, 1.63 mmol) and palladium on carbon (8.6 mg, 0.08 mmol) were suspended in 82 mL methanol. The flask for vacuumed and replaced with a hydrogen balloon. The reaction mixture was stirred at rt for 3 h. The solution was then filtered through a celite bed and the filtrate was concentrated to provide the bis-MOM protected fluoromethyl ketone (0.74 g, 96%).

Step 4. To the bis-MOM fluoromethyl ketone compound (0.74 g, 1.56 mmol) dissolved in 15.6 mL THF, 48% HBr (1.10 mL, 6.24 mmol) was added and the resulting solution was heated at 50 °C for 1 h. The mixture was cooled to rt and then quenched by slow addition of 20 mL saturated sodium bicarbonate solution. The biphasic solution was then concentrated on the rotovap and the resulting residue was partitioned using 20 mL DCM and 20 mL water. The

organic layer was separated and the aqueous layer was extracted with DCM (2 x 20 mL). The combined organic layers were then dried over sodium sulfate, filtered and concentrated. The crude compound was then purified by silica gel chromatography (40% ethyl acetate/60% hexanes to 60% ethyl acetate/40% hexanes) to provide the pure compound **7** (0.18 g, 29%) as a white foam.

Compound 7. TLC (Ethyl acetate:Hexanes, 70:30 v/v): $R_f = 0.36$; ^{1}H NMR (400 MHz, $CDCl_3$): δ 4.79 (d, J = 48.0 Hz, 1H), 3.85 (s, 1H), 3.50-3.44 (m, 1H), 2.60-2.44 (m, 2H), 2.20 (q. J = 13.2 Hz, 1H), 2.00-1.11 (m, 26H), 1.02-0.88 (m, 6H), 0.66 (s, 3H); ^{13}C NMR (100 MHz, $CDCl_3$): δ 207.62 (d, J = 19.2 Hz), 84.91 (d, J = 184.2), 71.98, 68.49, 55.70, 50.45, 42.69, 41.47, 39.88, 39.61, 39.41, 35.31, 35.24, 35.11, 35.03, 34.63, 32.83, 30.66, 28.67 (d, J = 1.7 Hz), 28.12, 23.68, 22.74, 20.56, 18.38, 11.76; HRMS (*m/z*): $[M - 2H_2O + H]^+$ calcd. for $C_{25}H_{41}FO_3$, 373.2907; found, 373.2888.

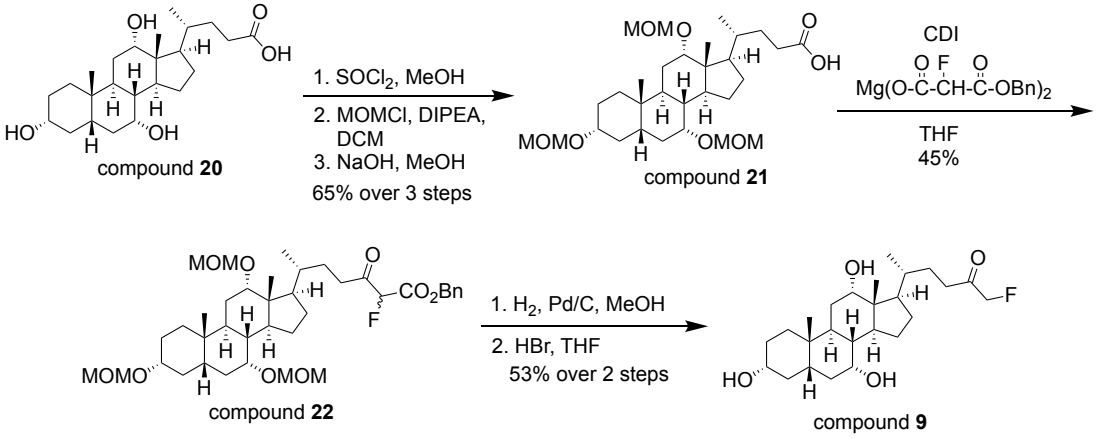

Scheme 5. Synthesis of Compound 9.

Compound **9** was synthesized from cholic acid (**20**) as per the procedure described above for compound **7**. Yields for the synthesis of compound **9** are listed in the scheme above.

Compound 9. TLC (100% Ethyl acetate): R_f = 0.12; ^{1}H NMR (400 MHz, $CDCl_3$): δ 4.80 (d, *J* = 47.6 Hz, 1H), 3.96 (s, 1H), 3.85 (s, 1H),3.48-3.41 (m, 1H), 2.63-2.43 (m, 2H), 2.27-1.25 (m, 24H), 1.17-1.07 (m, 1H), 1.02-0.94 (m, 4H), 0.89 (s, 3H), 0.68 (s, 3H); ^{13}C NMR (100 MHz, $CDCl_3$): δ 207.61 (d, *J* = 19.0 Hz), 84.92 (d, *J* = 184.2 Hz), 72.98, 71.92, 68.41, 46.97, 46.47, 41.82, 41.43, 39.65, 39.53, 35.21, 35.12, 35.07, 34.70, 34.63, 30.47, 28.60 (d, *J* = 1.5 Hz), 28.29, 27.43, 26.52, 23.18, 22.48, 17.44, 12.50; HRMS (*m/z*): $[M - 2H_2O + H]^+$ calcd. for $C_{25}H_{41}FO_4$, 371.2750; found, 371.2725.

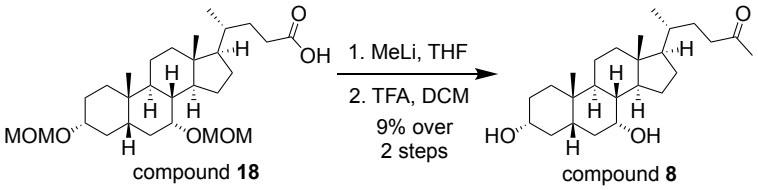

Scheme 6. Synthesis of compound 8.

Step 1. In a flame dried flask, the C-24 acid **18** (0.36 g, 0.75 mmol) was dissolved in 7.5 mL anhydrous THF and cooled to -5 °C. Methyllithium (1.35 mL, 2.24 mmol) was then added dropwise and the reaction was stirred at -5 °C for 1 h. The reaction was quenched with 8 mL water and concentrated on the rotovap. The residue was then partitioned using ethyl acetate and water. The organic layer was separated and the aqueous layer was extracted with ethyl acetate (2 x 10 mL). The combined organic layers were then dried over sodium sulfate, filtered and concentrated. The crude compound was then purified by silica gel chromatography (30% ethyl acetate/70% hexanes) to provide the pure compound (0.15 g, 42%) as a white foam.

Step 2. Compound **8**, was synthesized following step 3 as described above for compound **4**. The overall yield is reported on the reaction scheme.

Compound 8. TLC (Ethyl acetate:Hexanes, 30:70 v/v): Rf = 0.1; ^{1}H NMR (400 MHz, $CDCl_3$): δ 3.844-3.837 (m, 1H), 3.49-3.41 (m, 1H), 2.49-2.13 (m, 5H), 2.00-1.59 (m, 9H), 1.52-1.05 (m, 16H), 1.01-0.90 (m, 7H), 0.65 (s, 3H); ^{13}C NMR (100 MHz, $CDCl_3$): δ 209.66, 71.99, 68.50, 55.78, 50.45, 42.67, 41.47, 40.58, 39.88, 39.41, 35.31, 35.25, 35.03, 34.62, 32.83, 30.65, 29.87, 29.77, 28.15, 23.69, 22.75, 20.56, 18.41, 11.76 (one carbon overlapping with $CDCl_3$); HRMS (*m/z*): $[M - 2H_2O + H]^+$ calcd. for $C_{25}H_{42}O_3$, 355.3001; found, 355.2980.

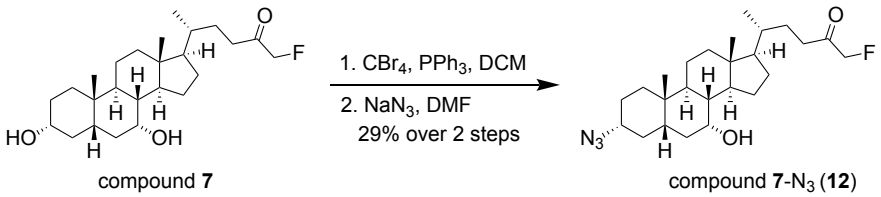

Scheme 7. Synthesis of compound 7-N_3 (12).

Step 1. To compound **7** (20.0 mg, 0.05 mmol) in 1 mL anhydrous DCM, triphenylphosphine (16.0 mg, 0.06 mmol) and carbon tetrabromide (21.0 mg, 0.06 mmol) were added and the reaction was stirred at rt for 18 h. The reaction was concentrated on the rotovap. The crude compound was then purified by silica gel chromatography (20% ethyl acetate/80% hexanes) to provide the pure bromide (15.0 mg, 65%) as a white powder.

Step 2. C-3 bromo compound (15.0 mg, 0.03 mmol), was dissolved in 0.5 mL DMF followed by the addition of sodium azide (4.1 mg, 0.06 mmol). The reaction mixture was heated at 100 °C for 1 h. The mixture was concentrated on the rotovap and partitioned using saturated solution of sodium bicarbonate and ethyl acetate (5 mL each). The organic layer was separated and the aqueous layer was extracted with ethyl acetate (2 x 5 mL). The combined organic layers were then dried over sodium sulfate, filtered and concentrated. The crude compound was then purified by silica gel chromatography (20% ethyl acetate/80% hexanes) to provide the pure

compound **7**-N_3 (6.0 mg, 44%) as a white powder. The overall yield is reported on the reaction scheme.

Compound 7-N_3 (12). TLC (Ethyl acetate:Hexanes, 30:70 v/v): Rf = 0.56; ^{1}H NMR (400 MHz, $CDCl_3$): δ 4.81 (d, *J* = 38.4 Hz, 2H), 3.87 (s, 1H), 3.20-3.13 (m, 1H), 2.63-2.45 (m, 2H), 2.37 (q, *J* = 10.4 Hz, 1H), 2.06-1.62 (m, 9H), 1.53-1.14 (m, 14H), 1.04-0.90 (m, 7H), 0.69-0.65 (m, 3H); ^{13}C NMR (125 MHz, DMSO-d_6): δ 209.29 (d, *J* = 15.0 Hz), 87.90 (d, *J* = 178.8 Hz), 69.15, 63.79, 58.48, 53.07, 45.04, 44.50, 43.56, 38.15, 38.11, 37.90, 37.80, 37.58, 36.88, 35.36, 31.46, 30.83, 29.57, 26.21, 25.74, 23.35, 21.44, 14.80 (one carbon signal may overlap with DMSO); HRMS (*m/z*): $[M + Na]^+$ calcd. for $C_{25}H_{40}FN_3O_2$, 456.3002; found, 456.2985.

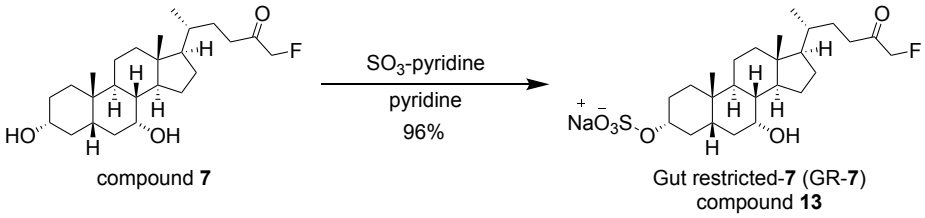

Scheme 8. Synthesis of GR-7 (compound 13).

To compound **7** (60.0 mg, 0.15 mmol) dissolved in 4 mL pyridine, SO_3.pyridine (70.1 g, 0.44 mmol) was added and the resulting solution was stirred at rt for 18 h. The reaction mixture was concentrated on a rotovap. The resulting slurry was resuspended in 10:1 dichloromethane:methanol (10 mL) and washed with 10 mL saturated solution of sodium bicarbonate. The organic layer was separated and the aqueous layer was extracted with 10:1 dichloromethane:methanol (10 mL). The combined organic layer was re-subjected to the above extraction process. The obtained organic layer was dried over sodium sulfate, filtered and concentrated. The crude compound was then purified by silica gel chromatography (80% dichloromethane/20% methanol) to provide pure GR-**7** (69.0 mg, 96%) as a white powder.

GR-7 (compound 13). TLC (Dichloromethane:Methanol, 80:20 v/v): Rf = 0.39; ^{1}H NMR (400 MHz, CD_3OD): δ 4.91 (d, *J* = 47.6 Hz, 2H), 4.17-4.10 (m, 1H), 3.78 (d, *J* = 1.2 Hz, 1H), 2.79 (br s, 0.4H), 2.59-2.37 (m, 3H), 2.00-1.70 (m, 9H), 1.56-0.93 (m, 20H), 0.69 (s, 3H); ^{13}C NMR (100 MHz, CD_3OD): δ 207.69 (d, *J* = 16.9 Hz), 84.50 (d, *J* = 181.0 Hz), 79.30, 67.56, 55.74, 50.06, 42.22, 41.85, 39.56, 39.31, 36.32, 35.24, 35.03, 34.71, 34.38, 34.01, 32.57, 28.57, 27.776, 27.64, 23.18, 21.84, 20.35, 17.48, 10.70; HRMS (*m/z*): $[M - H]^-$ calcd. for $C_{25}H_{40}FO_6S$, 487.2535; found, 487.2532.

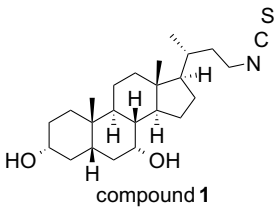
S
C
N
H
H
H
H
HO
H
OH

compound **1**

3.830
3.574
3.411
2.236
2.205
2.174
2.143
1.993
1.791
1.714
1.679
1.671
1.641
1.566
1.550
1.108
1.003
0.997
0.891
0.668
9.5 9.0 8.5 8.0 7.5 7.0 6.5 6.0 5.5 5.0 4.5 4.0 3.5 3.0 2.5 2.0 1.5 1.0 ppm
1.00
2.96
1.11
7.59
3.45
15.10
7.38
3.04

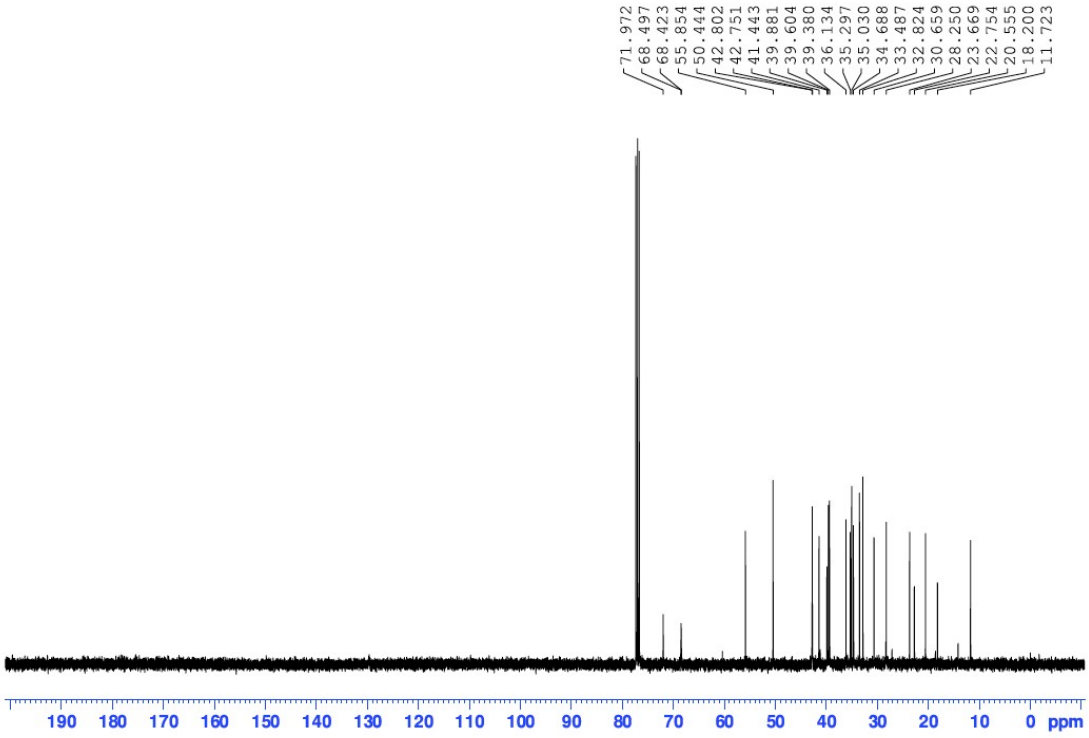
71.972
68.497
68.423
55.854
50.444
42.802
42.751
41.443
39.881
39.604
39.380
36.134
35.297
35.030
34.688
33.487
32.824
30.659
28.250
23.669
22.754
20.555
18.200
11.723
190 180 170 160 150 140 130 120 110 100 90 80 70 60 50 40 30 20 10 0 ppm

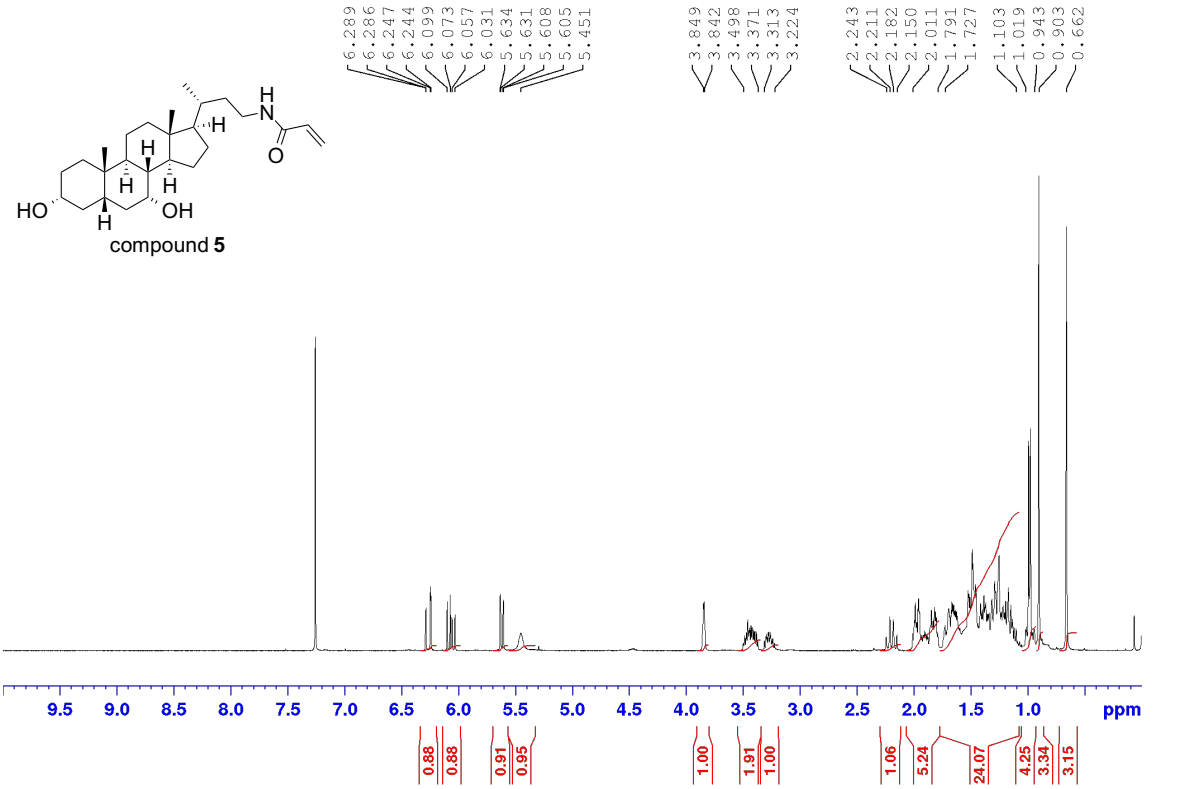
6.289
6.286
6.247
6.244
6.099
6.073
6.057
6.031
5.634
5.631
5.608
5.605
5.451
3.849
3.842
3.498
3.371
3.313
3.224
2.243
2.211
2.182
2.150
2.011
1.791
1.727
1.103
1.019
0.943
0.903
0.662
HO
OH
H
N
O
compound 5
9.5 9.0 8.5 8.0 7.5 7.0 6.5 6.0 5.5 5.0 4.5 4.0 3.5 3.0 2.5 2.0 1.5 1.0 ppm
0.88
0.88
0.91
0.95
1.00
1.91
1.00
1.06
5.24
24.07
4.25
3.34
3.15

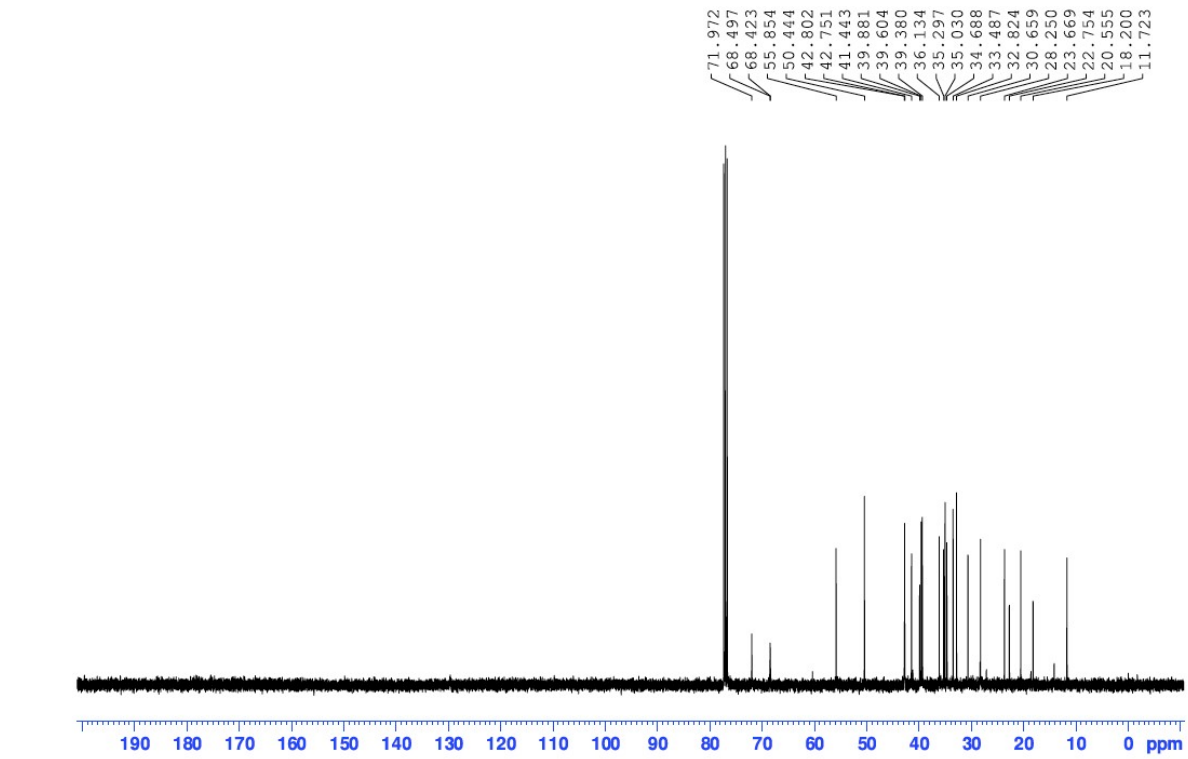
71.972
68.497
68.423
55.854
50.444
42.802
42.751
41.443
39.881
39.604
39.380
36.134
35.297
35.030
34.688
33.487
32.824
30.659
28.250
23.669
22.754
20.555
18.200
11.723
190 180 170 160 150 140 130 120 110 100 90 80 70 60 50 40 30 20 10 0 ppm

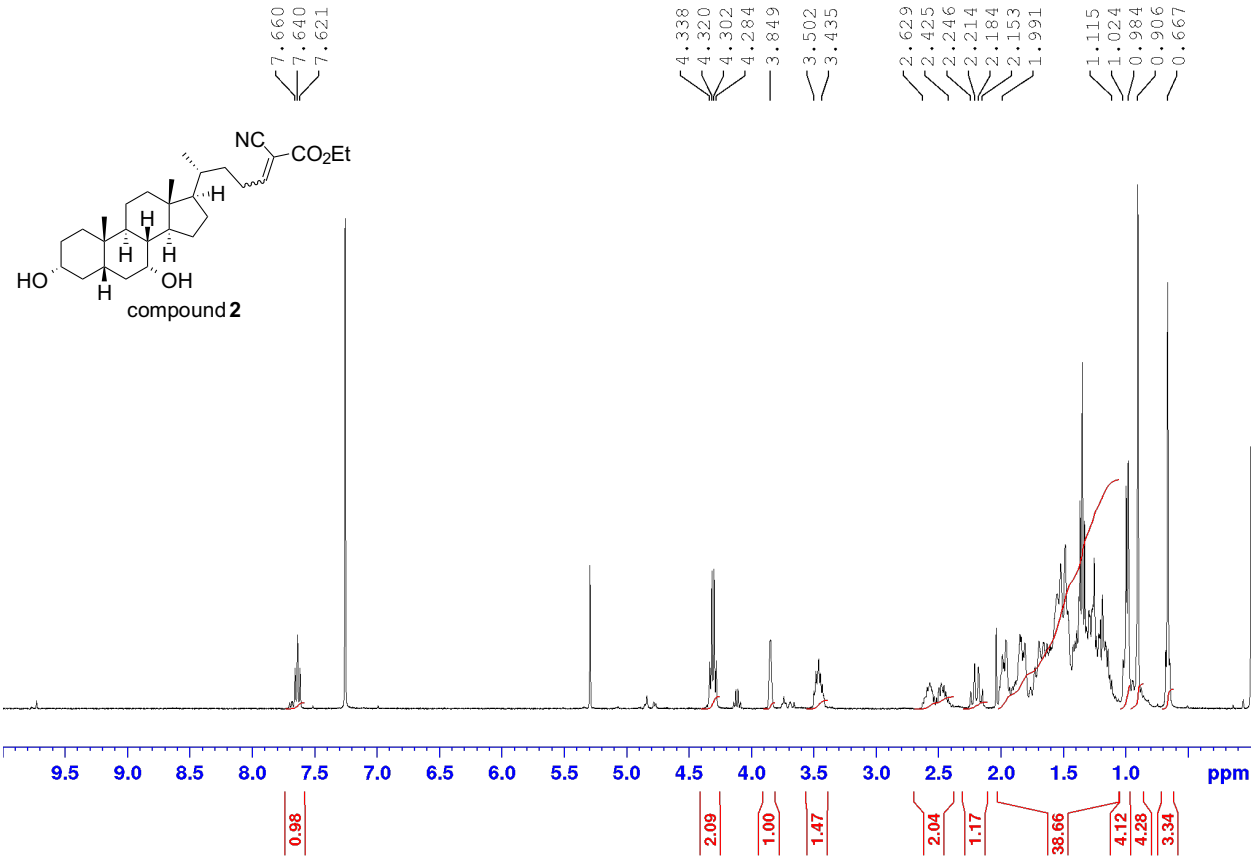
7.660
7.640
7.621
4.338
4.320
4.302
4.284
3.849
3.502
3.435
2.629
2.425
2.246
2.214
2.184
2.153
1.991
1.115
1.024
0.984
0.906
0.667
NC
CO2Et
H
H
H
H
HO
OH
H
compound 2
9.5
9.0
8.5
8.0
7.5
7.0
6.5
6.0
5.5
5.0
4.5
4.0
3.5
3.0
2.5
2.0
1.5
1.0
ppm
0.98
2.09
1.00
1.47
2.04
1.17
38.66
4.12
4.28
3.34

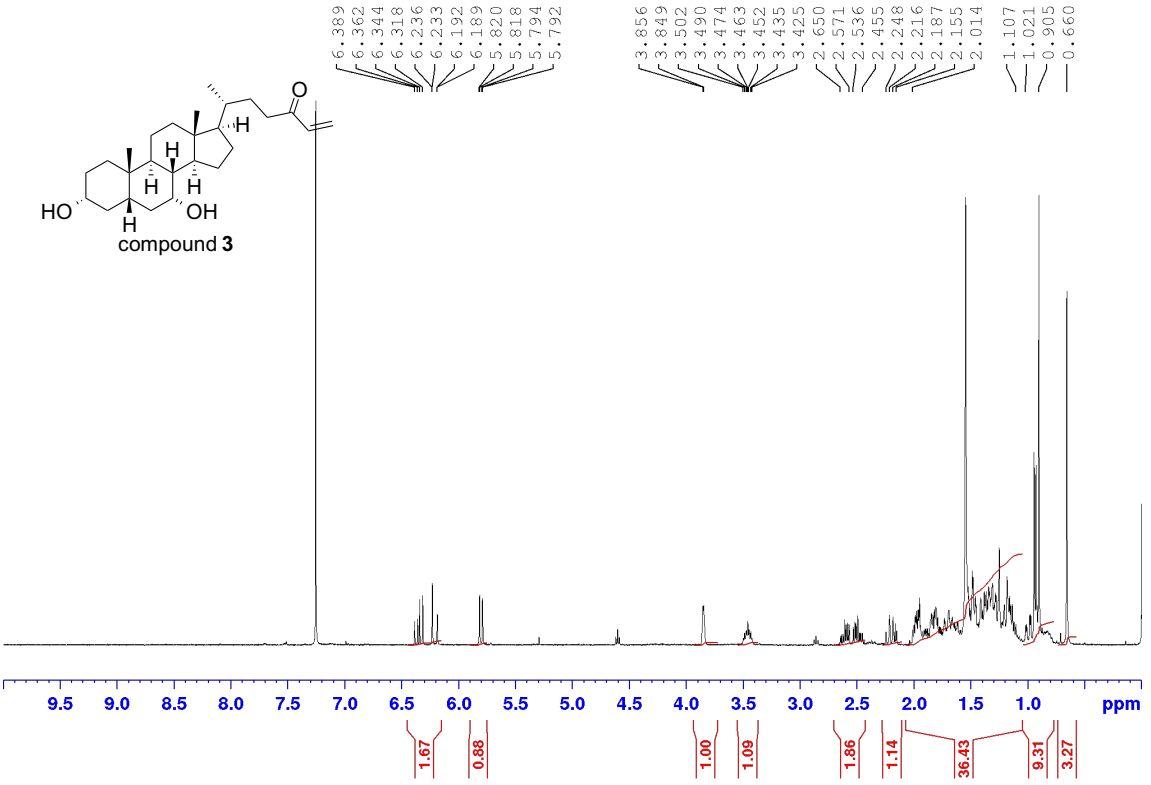
6.389
6.362
6.344
6.318
6.236
6.233
6.192
6.189
5.820
5.818
5.794
5.792
3.856
3.849
3.502
3.490
3.474
3.463
3.452
3.435
3.425
2.650
2.571
2.536
2.455
2.248
2.216
2.187
2.155
2.014
1.107
1.021
0.905
0.660
O
H
H
H
H
HO
OH
H
compound 3
9.5 9.0 8.5 8.0 7.5 7.0 6.5 6.0 5.5 5.0 4.5 4.0 3.5 3.0 2.5 2.0 1.5 1.0 ppm
1.67
0.88
1.00
1.09
1.86
1.14
36.43
9.31
3.27

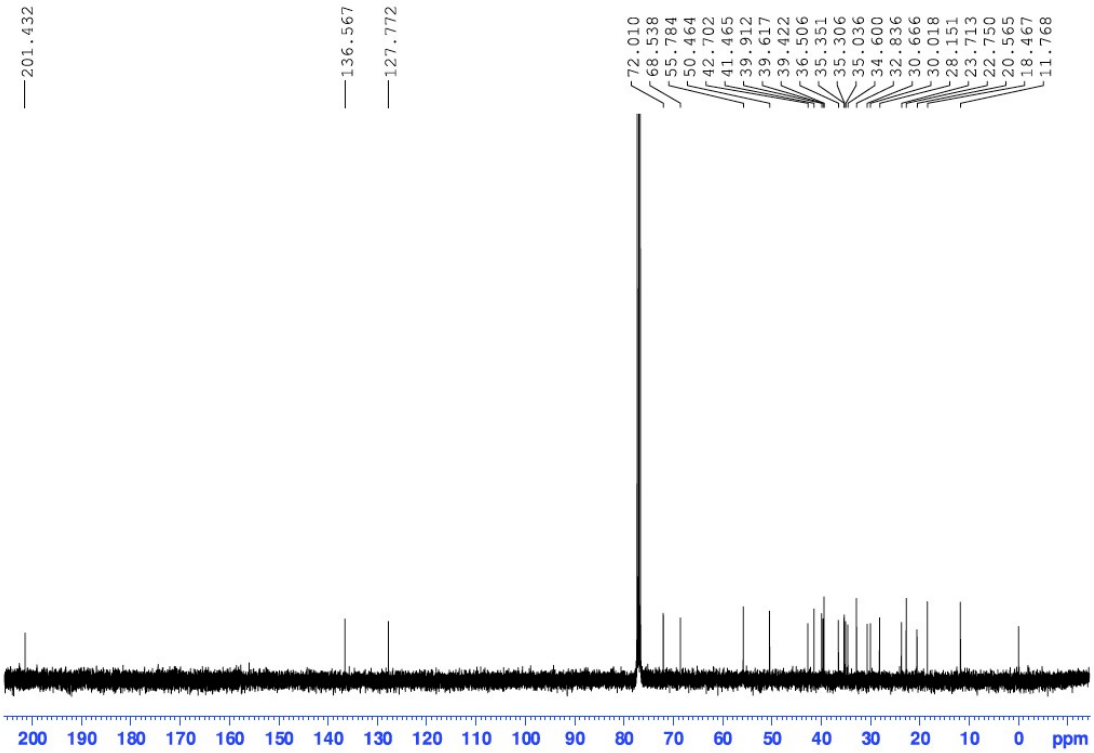
201.432
136.567
127.772
72.010
68.538
55.784
50.464
42.702
41.465
39.912
39.617
39.422
36.506
35.351
35.306
35.036
34.600
32.836
30.666
30.018
28.151
23.713
22.750
20.565
18.467
11.768
200 190 180 170 160 150 140 130 120 110 100 90 80 70 60 50 40 30 20 10 0 ppm

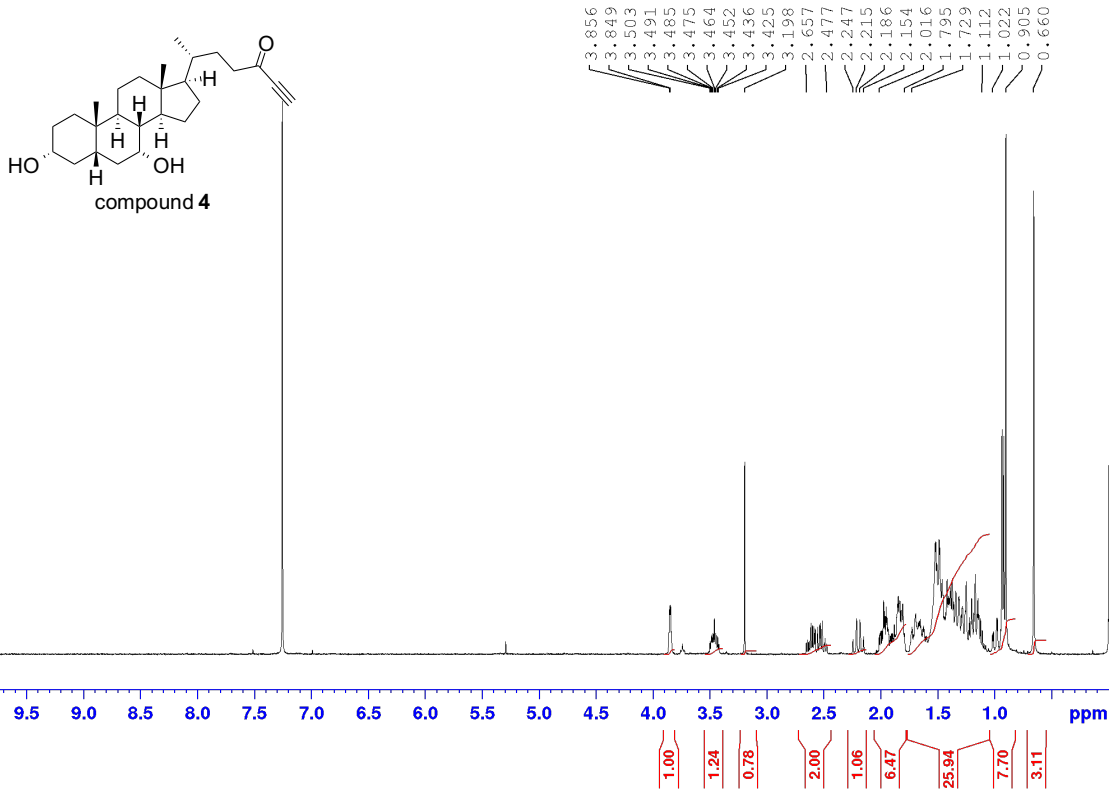
3.856
3.849
3.503
3.491
3.485
3.475
3.464
3.452
3.436
3.425
3.198
2.657
2.477
2.247
2.215
2.186
2.154
2.016
1.795
1.729
1.112
1.022
0.905
0.660
O
H
H
H
H
HO
OH
H
9.5 9.0 8.5 8.0 7.5 7.0 6.5 6.0 5.5 5.0 4.5 4.0 3.5 3.0 2.5 2.0 1.5 1.0 ppm
1.00
1.24
0.78
2.00
1.06
6.47
25.94
7.70
3.11

compound **4**

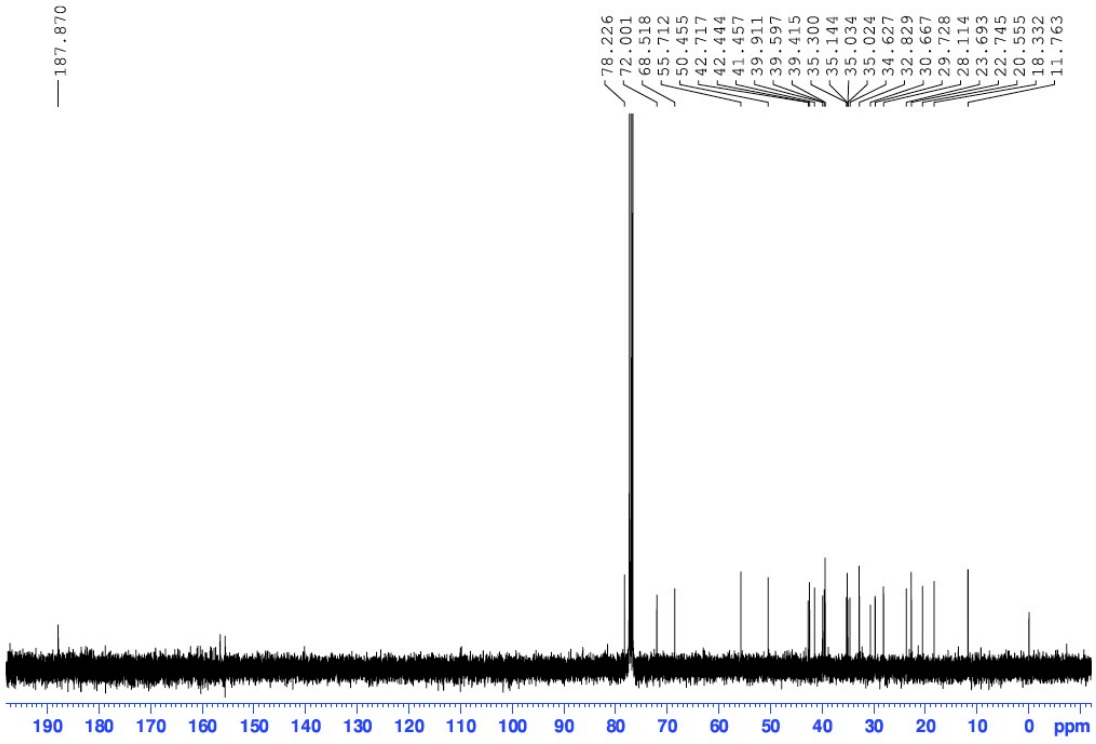
187.870
78.226
72.001
68.518
55.712
50.455
42.717
42.444
41.457
39.911
39.597
39.415
35.300
35.144
35.034
35.024
34.627
32.829
30.667
29.728
28.114
23.693
22.745
20.555
18.332
11.763
190 180 170 160 150 140 130 120 110 100 90 80 70 60 50 40 30 20 10 0 ppm

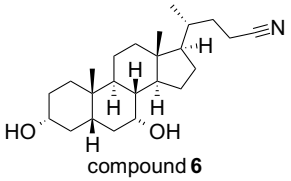
N
H
H
H
H
HO
OH
H

compound **6**

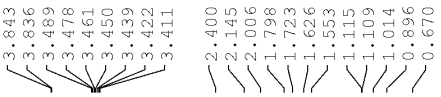
3.843
3.836
3.489
3.478
3.461
3.450
3.439
3.422
3.411
2.400
2.145
2.006
1.798
1.723
1.626
1.553
1.115
1.109
1.014
0.896
0.670

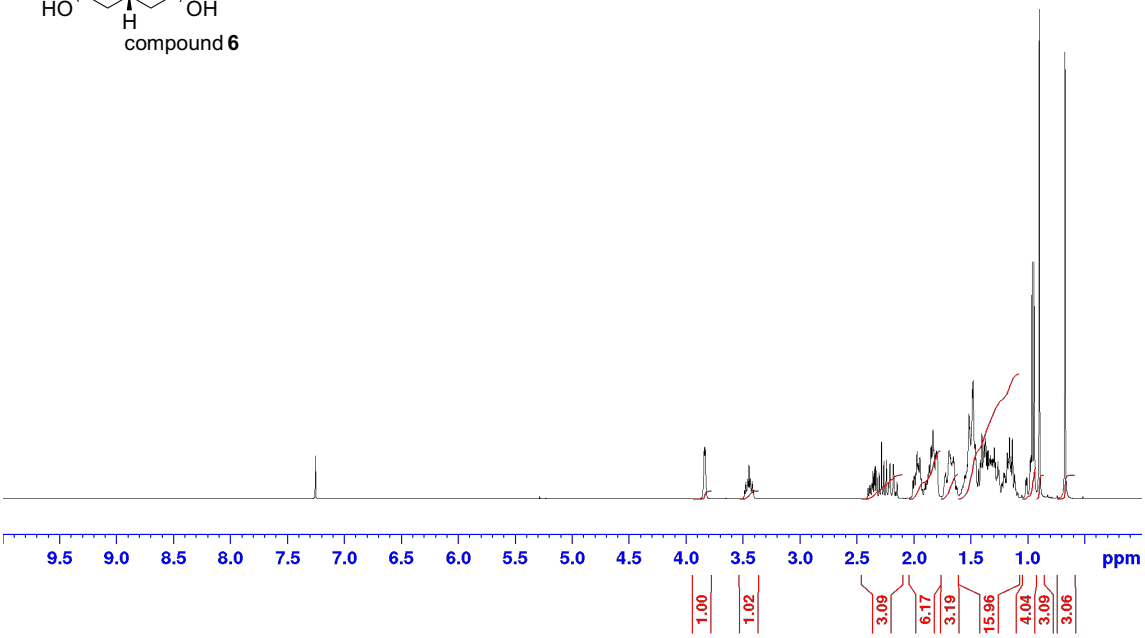
9.5
9.0
8.5
8.0
7.5
7.0
6.5
6.0
5.5
5.0
4.5
4.0
3.5
3.0
2.5
2.0
1.5
1.0
ppm
1.00
1.02
3.09
6.17
3.19
15.96
4.04
3.09
3.06

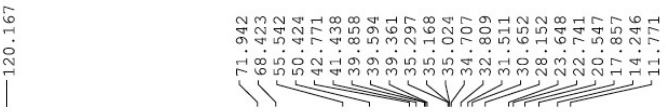
120.167
71.942
68.423
55.542
50.424
42.771
41.438
39.858
39.594
39.361
35.297
35.168
35.024
34.707
32.809
31.511
30.652
28.152
23.648
22.741
20.547
17.857
14.246
11.771

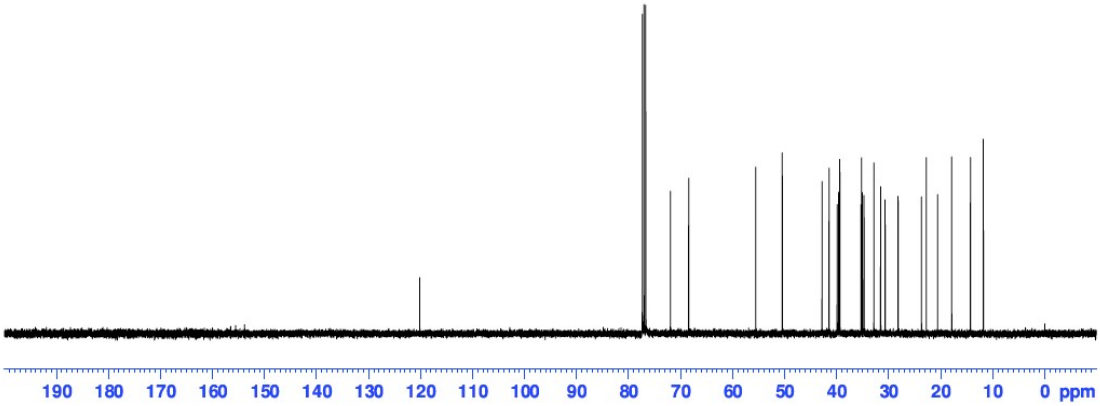
190
180
170
160
150
140
130
120
110
100
90
80
70
60
50
40
30
20
10
0 ppm

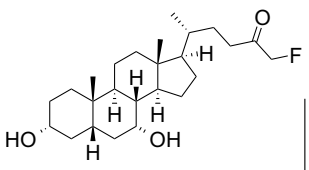
O
F
H
H
H
H
HO
OH
H

compound **7**

4.853
4.733
3.852
3.500
3.491
3.475
3.464
3.452
3.436
2.598
2.442
2.248
2.215
2.186
2.151
2.003
1.110
1.021
1.014
0.881
0.661
9.5 9.0 8.5 8.0 7.5 7.0 6.5 6.0 5.5 5.0 4.5 4.0 3.5 3.0 2.5 2.0 1.5 1.0 ppm
1.41
1.00
0.92
1.54
1.10
32.03
6.79
2.60

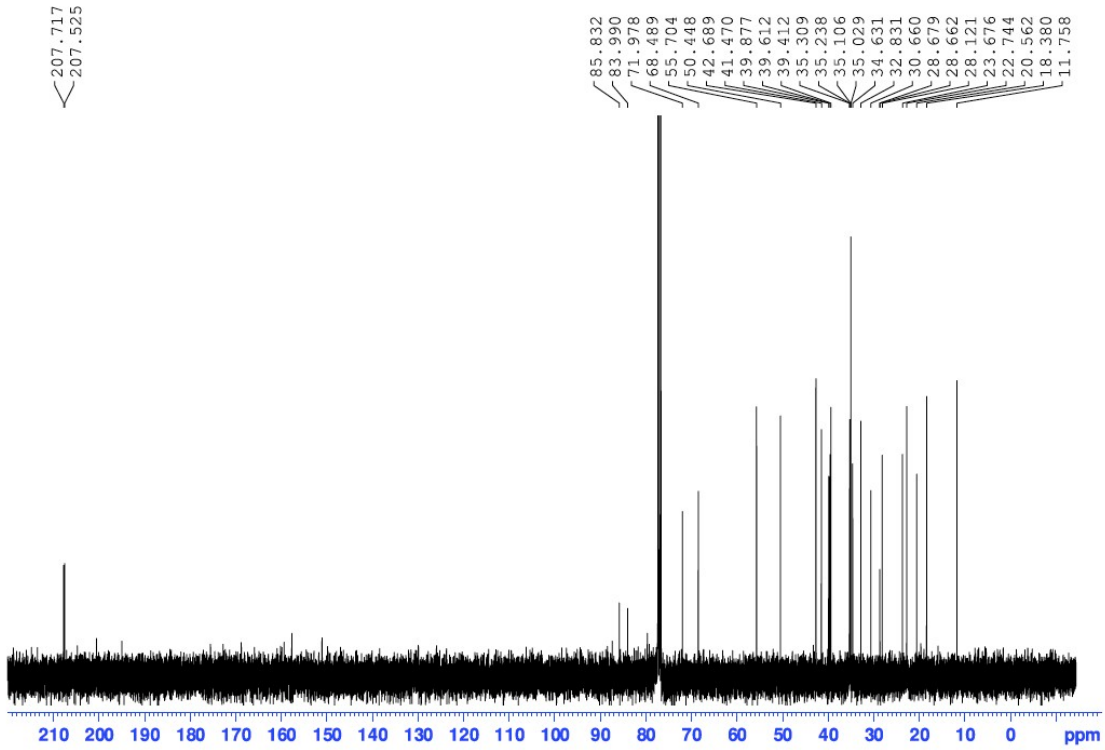
207.717
207.525
85.832
83.990
71.978
68.489
55.704
50.448
42.689
41.470
39.877
39.612
39.412
35.309
35.238
35.106
35.029
34.631
32.831
30.660
28.679
28.662
28.121
23.676
22.744
20.562
18.380
11.758
210 200 190 180 170 160 150 140 130 120 110 100 90 80 70 60 50 40 30 20 10 0 ppm

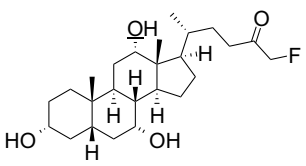
OH
O
H
F
H
H
H
HO
OH
H

compound **9**

4.856
4.737
3.962
3.848
3.476
3.459
3.448
3.438
3.421
3.410
2.633
2.430
2.269
1.249
1.173
1.068
1.015
0.937
0.887
0.679
9.5
9.0
8.5
8.0
7.5
7.0
6.5
6.0
5.5
5.0
4.5
4.0
3.5
3.0
2.5
2.0
1.5
1.0
ppm
0.74
0.75
0.94
1.30
1.00
1.65
24.10
1.14
3.95
3.06
3.08

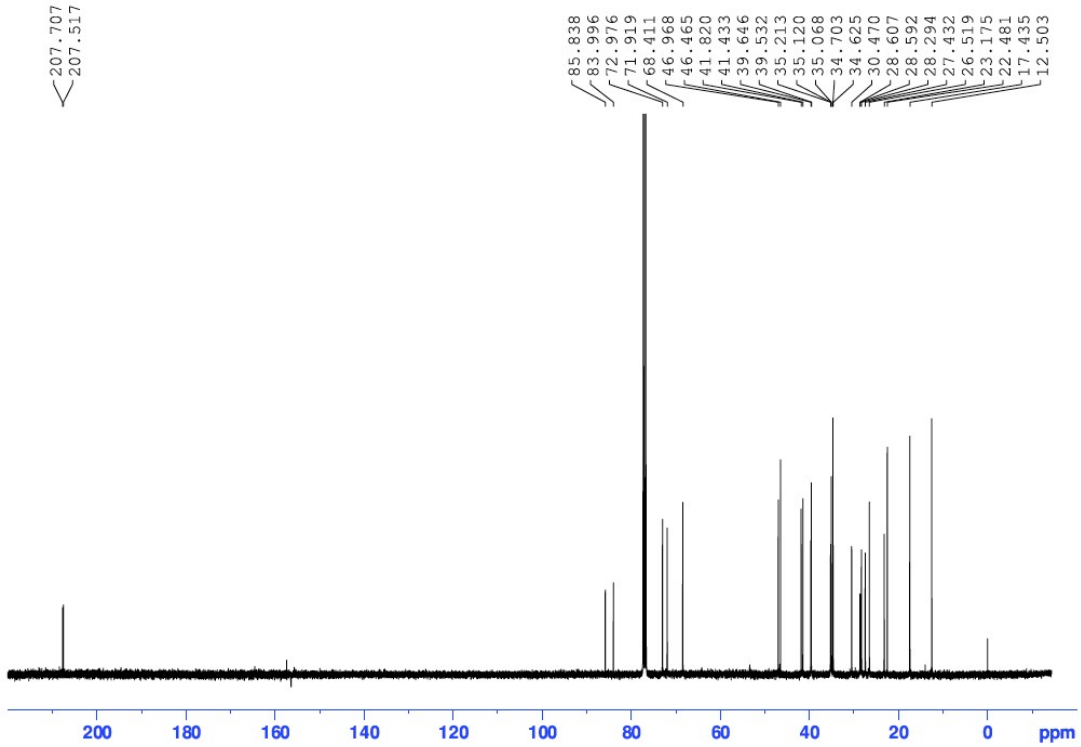
207.707
207.517
85.838
83.996
72.976
71.919
68.411
46.968
46.465
41.820
41.433
39.646
39.532
35.213
35.120
35.068
34.703
34.625
30.470
28.607
28.592
28.294
27.432
26.519
23.175
22.481
17.435
12.503
200
180
160
140
120
100
80
60
40
20
0
ppm

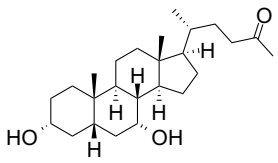
O
H
H
H
H
HO
OH
H

compound **8**

3.844
3.837
3.492
3.481
3.464
3.453
3.442
3.425
3.414
2.485
2.405
2.367
2.286
2.246
2.214
2.185
2.152
2.129
2.002
1.597
1.590
1.520
1.050
1.011
0.913
0.896
0.647
9.5 9.0 8.5 8.0 7.5 7.0 6.5 6.0 5.5 5.0 4.5 4.0 3.5 3.0 2.5 2.0 1.5 1.0 ppm
1.00
1.02
0.99
1.07
3.90
9.50
16.42
7.46
3.11

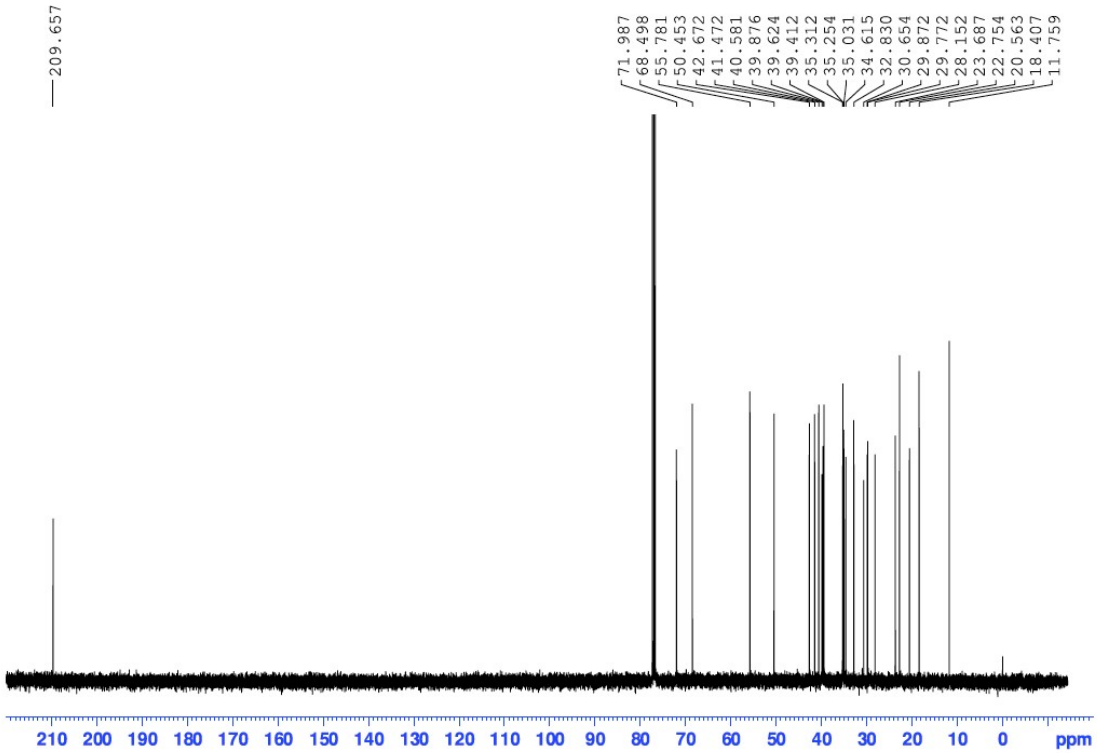
209.657
71.987
68.498
55.781
50.453
42.672
41.472
40.581
39.876
39.624
39.412
35.312
35.254
35.031
34.615
32.830
30.654
29.872
29.772
28.152
23.687
22.754
20.563
18.407
11.759
210 200 190 180 170 160 150 140 130 120 110 100 90 80 70 60 50 40 30 20 10 0 ppm

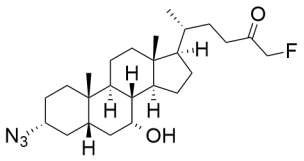

compound **7**-N_3 (**12**)

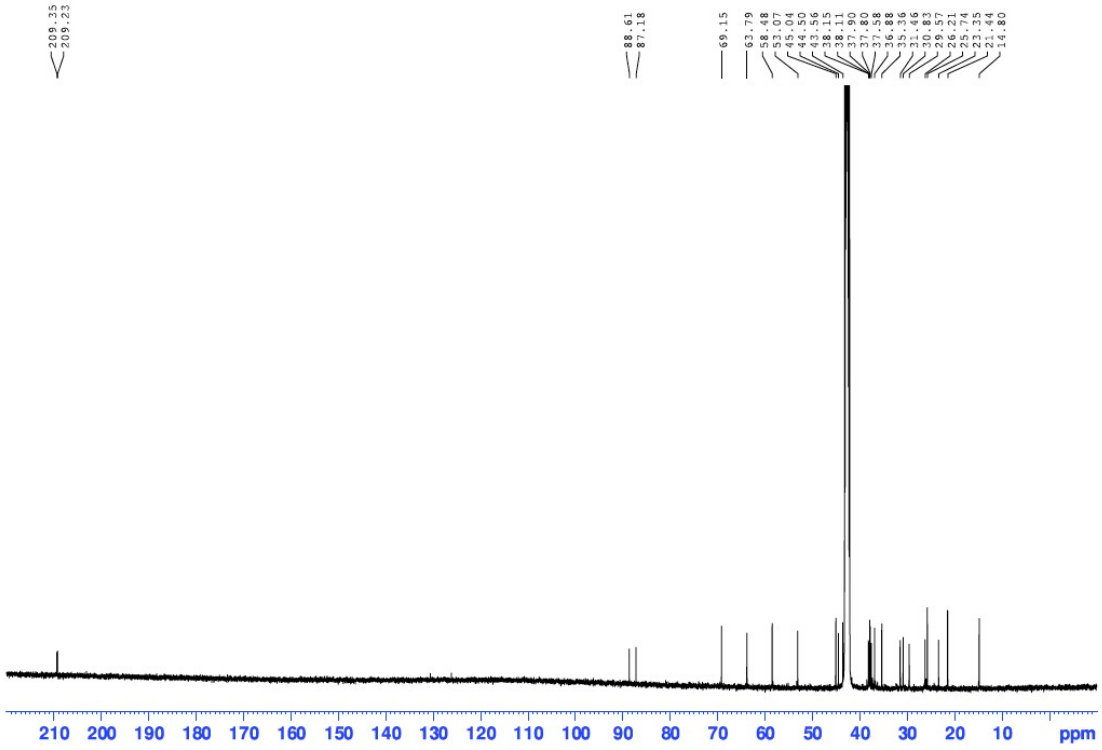

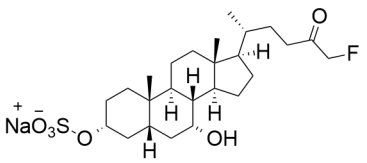

Gut restricted-**7** (GR-**7**)
compound **13**